EFFECTS OF SURFACE ANOMALIES ON CERTAIN MODEL-GENERATED METEOROLOGICAL HISTORIES

Jerome Spar

Prepared under
Grant NGR 33-016-174
Goddard Space Flight Center,
NASA

New York University
School of Engineering and Science
University Heights, New York, N.Y. 10453
Department of Meteorology and Oceanography
Geophysical Sciences Laboratory Report No. GSL-[illegible]-2

Research Division

April 1972

New York University
School of Engineering and Science
Department of Meteorology and Oceanography

EFFECTS OF SURFACE ANOMALIES ON CERTAIN MODEL-GENERATED METEOROLOGICAL HISTORIES

Jerome Spar

Prepared under
Grant NGR 33-016-174
for
Goddard Space Flight Center NASA

April 1972

Acknowledgements

The author gratefully acknowledges the hospitality and services provided by Dr. Robert Jastrow and the staff of the Goddard Institute for Space Studies, without whom this work would not have been possible. The cooperation and assistance of Dr. Milton Halem, who arranged for computing facilities, is especially appreciated. Mr. John Liu was responsible for all the programming and computations carried out for the project on the GISS IBM 360/95 computer. His services were invaluable. We also wish to thank Professors Y. Mintz and A. Arakawa of the University of California, Los Angeles, for graciously allowing us to use their model and programs for these experiments. Mrs. Shu-hsien Chow performed the spectral analyses and contributed to the study of the SNW experiment at New York University.

Abstract

The Mintz-Arakawa 2-level general circulation model has been used in a series of experiments to compute the response of the model atmosphere to (1) a positive sea surface temperature (SST) anomaly in the North Pacific Ocean in summer and in winter, (2) an identical anomaly in the South Pacific Ocean in the Southern Hemisphere winter, and (3) anomalous northward and southward displacements of the Northern Hemisphere snow line over the continents. In each case computations were carried out for 90 "forecast" days. Results are shown in terms of the differences between anomaly and control histories. Time series of certain regional response indices, including area-average sea level pressure and 600 mb circulation indices, as well as 30-day mean sea level pressure maps are used in the analysis. Of particular interest is the evidence of significant interhemisphere influence.

Introduction

The development of computationally stable general circulation models (see, e.g., Mintz, 1956; Smagorinsky, et al., 1965; Leith, 1965; Kasahara and Washington, 1967; Holloway and Manabe, 1971) appears to have opened the way for some preliminary experimentation in dynamical long range weather prediction. A direct operational attack on the long range forecasting problem by extended time integrations of general circulation models would obviously be premature at this time. However, models may provide at least tentative answers to certain basic questions related to long range forecasting.

Some physical problems which may be investigated with models are the long-term effects on the atmosphere of anomalies in sea surface temperature, sea ice, and snow cover, the role of interhemispheric exchange, and the possible influences of such phenomena as volcanic dust and solar variations. Among the computational problems which can be studied are the effects of horizontal grid size and vertical resolution on the predicted atmospheric histories. Another basic problem of long range weather prediction that can be approached through models is the influence of the initial state of the atmosphere on its evolution over periods of a month or more, and the degree of specification and resolution of the initial state required for long range forecasting. Only a few of these problems are examined in this paper.

For many years meteorologists have sought a physical basis for long range weather prediction. One hypothesis which has been proposed by several workers in the field is that the atmosphere exhibits certain long-term responses to anomalous surface conditions. Anomalies in sea ice, snow cover, and sea surface temperature have been proposed as possible causes of subsequent atmospheric anomalies. During the past decade, for example, J. Namias has published a series of papers (see, e.g., Namias, 1962) in which he has noted the occasional persistence of large sea surface temperature anomalies, and has speculated on their possible influence on the atmosphere over months, seasons, and even years (Namias, 1969). In a recent study of large-scale air-sea

interactions (Namias, 1971) he has described some possible effects of anomalously warm sea surface temperatures in the Pacific Ocean on subsequent weather patterns over the Northern Hemisphere. Similar views have also been put forth by J. Bjerknes (1966, 1969) particularly with respect to the possible remote effects of sea surface temperature anomalies in the equatorial Pacific.

Because of the strong interactions between the atmosphere and the earth's surface, long range weather prediction must eventually seek to account for the variations in the total, coupled earth-atmosphere system over the forecast period[1]. However, as Namias (1970) has noted, sea surface temperature anomalies, once established, may persist for a long time thereafter, despite interactions with the atmosphere. In such cases it may be possible to calculate the effects of these persistent surface anomalies on the subsequent behavior of the atmosphere even with a non-interactive general circulation model.

A set of experiments in simulated long range prediction has been carried out at the Goddard Institute for Space Studies (GISS) with the global, two-level general circulation model developed by Y. Mintz and A. Arakawa at the University of California (UCLA). (See references below.) In these experiments certain hypothetical persistent anomalies in sea surface temperature and in snow cover were introduced, and the model was run for "forecast periods" up to 3 months. The response of the model atmosphere to the anomalies was evaluated by comparing the results of these runs with "control" runs based on identical conditions except for the absence of the surface anomalies. The predictions are

---

[1] A joint ocean-atmosphere general circulation model, which has been used only for the calculation of an equilibrium climate, has been described by Manabe and Bryan (1969). Interactions between the atmosphere and the earth's surface hydrology, including the sea surface, pack ice, snow cover and soil moisture, are included in the Manabe-Bryan model. However, the application of such a joint model to practical weather prediction still seems remote.

"simulated" in the sense that the initial states (as well as the subsequent histories) are model-generated rather than real.

Comparisons of the "control" and "anomalous" runs are presented below in terms of various indices of response, including both monthly mean values and certain measures of variability. Long range forecasts have usually been limited to the prediction of mean values over some long forecast period, e.g., a month, or a season. However, it is not at all certain that time averages (e.g., monthly mean pressure or geopotential fields, or monthly mean temperature anomalies) are the best goals, or are even attainable goals, for long range weather forecasting. Quite possibly the variability of the atmosphere over some forecast period may be at least as useful and even more readily predictable than time averages. For example, the response of the atmosphere to certain surface anomalies may take the form of a shift in storm track, or a change in the rate of cyclogenesis, or some other synoptic characteristics. If so, the atmospheric response may not be apparent in, say, the local 30-day mean values, but may show up in the form of a change in regional variability. For this reason, certain regional response indices, which presumably reflect the variability associated with cyclone passages and other synoptic activity, were used in an effort to evaluate the long term effects of surface anomalies on the model atmosphere. These are described below.

It must be emphasized that these experiments are not directly relevant to the problem of the inherent predictability of the atmosphere. It is quite possible that the effects of random error or of random variations in initial state, which have been demonstrated in numerous extended forecast experiments (e.g., see Charney, et al., 1966), may overwhelm any effects due to systematic anomaly fields such as those studied here. These experiments only indicate what the effects of certain organized anomalies in surface parameters may be. They do not suggest that, given such anomalies, one can predict the future state of the atmosphere any better than one can predict the state of the atmosphere when these anomalies are absent. Thus, the problem

of predictability, per se, is not the subject of this investigation. We are interested only in knowing what the specific contributions of the anomalies studied may be to the total variability of the atmosphere.

The general circulation model

The experiments described in this paper were carried out with the two-level, global general circulation model of Arakawa and Mintz. The two-level UCLA model originally devised by Mintz (1965) has undergone a series of modifications, and is now in the form described by Langlois and Kwok (1969), but with the treatment of radiation and convection as given by Arakawa, Katayama and Mintz (1968).

In brief, the model atmosphere, bounded by the earth's surface and the 200 mb level, is divided into two layers of equal mass. The horizontal velocity and temperature of the two layers, the water vapor in the lower layer, and the surface pressure are predicted from the primitive equations cast in "sigma-coordinates" on a spherical grid of 5° of longitude by 4° of latitude. The earth's surface is specified as open ocean of given surface temperature, or as bare land of given altitude, or as ice covered ocean, or ice or snow covered land. The model includes a water cycle (with clouds and precipitation), parameterized moist convection, radiation (including continuously varying solar distance, declination, and zenith angle), variable ground temperature (computed from a surface energy balance condition), and a prescribed seasonal variation in the latitude of the Northern Hemisphere snow line. The Arakawa differencing scheme, which satisfies the important integral constraints, allows the model to be run for long periods of time without degradation of its realistic-looking synoptic features. Started from an initial state of rest, the model generates a credible meteorological history, including a reasonable climatology and annual cycle (Katayama, Mintz, and Arakawa, 1971).

In the GISS experiments with the model, the generated history was interrupted and certain anomalies were inserted in the sea surface temperature field or in the mean latitude of the Northern Hemisphere

snow line. The subsequent evolution of the model atmosphere was then compared with a "control" history computed without anomalies. The response of the model atmosphere is the result of the alteration of the heat and moisture flux between the air and the underlying surface caused by either changes in sea surface temperature or changes in surface albedo and thermal properties associated with the presence or absence of a snow cover.

Response indices

The long-term response of the model atmosphere to any given stimulus can be measured in many different ways. In this study we have adopted the view that measures of response should be regional as well as global, that they should be related in some way to the requirements and expectations of long range weather forecasting, and that they should measure the effects of the stimulus on variability as well as on mean values.

Three regional indices of response chosen for the study were (1) a daily regional mean sea level pressure, P, over a 3-month period, (2) a daily regional zonal index, Z, at 600 mb over the 3-month period, and (3) a daily regional meridional index, M, at 600 mb over the 3-month period. In addition, global and regional synoptic maps of monthly mean sea level pressures were computed for each of three consecutive months after initial time, as well as for overlapping 30-day periods stepped at 10-day intervals.

The P index is computed as a daily space-time average sea level pressure (in millibars) over the eastern region of North America bounded by latitudes 30°N and 50°N and longitudes 70°W and 90°W. One value of P is computed for each day of a 3-month "forecast" period from the 2-hourly values of sea level pressure calculated on a 5 x 6 grid point array. The quantity P(t) may be thought of as an index of regional synoptic activity. For example, if the forecast period is characterized by frequent cyclone passages across the region, P may exhibit large changes from day to day, while if the cyclone tracks fall outside the region for

the most part, P may change relatively little during the forecast period.

The Z index is a measure of the strength of the geostrophic westerly wind. In this study Z is a regional index, measured between longitudes 50°W and 140°W (across North America), and is equal to the difference between the mean geopotential heights (in meters) at 30°N and 50°N at the 600 mb level. One daily time-averaged value of Z is calculated for each "forecast" day of the 3-month period from the 2-hourly gridpoint values generated by the model. Positive values of Z represent westerly geostrophic wind components. Small values of Z may, of course, represent either a condition of weak westerly circulation or of large amplitude waves.

The M index is a measure of the magnitude and sign of the meridional geostrophic wind component. This index is defined as the difference between the average 600 mb geopotential heights, measured from 30°N to 50°N, along the 70°W and 90°W meridians. Positive values of M signify lower heights to the west, and hence southerly geostrophic wind components, while negative values denote northerly geostrophic components. Passage of a north-south trough line from west to east across the eastern region of North America is indicated by a change in the sign of M from positive to negative. One daily time average of M is calculated for each "forecast" day of the 3-month period from the 2-hourly gridpoint values.

A 90-day time series of each index was generated by the model for each control case (one winter case and one summer case) and for each anomaly experiment. To provide a basis for comparison of each experimental (i.e., anomalous) run with its corresponding control run, certain spectra were also computed from the index time series. As a further aid in the comparison of anomaly and control runs, 3-month "difference series" were generated by computing the algebraic differences between the corresponding anomaly and control index values for each day. Difference maps were also computed from 30-day mean anomaly and control sea level pressure fields.

The model employed has been shown to reproduce the climatological pressure patterns of the atmosphere with a good degree of similitude. It has not yet been shown that similar success can be achieved in reproducing the cloud and precipitation climatology with the 2-level model, and indeed this seems unlikely. Therefore, no attempt has been made as yet to measure the atmospheric response to the various surface anomalies in terms of variables other than pressure (or geopotential). In this sense it may be said that the experiments described here are concerned with the "dynamical" response of the model atmosphere to surface anomalies, rather than with its "physical" response.

Experiments

Simulated predictions were computed for both the summer and winter seasons. In each experiment the run begins with the solar declination set close to its maximum or minimum value, depending on season. Both declination and solar distance then vary appropriately with calendar date during the 3-month forecast run. Initial conditions for the two sets of experiments were taken from history tapes generated by the UCLA model, which was started from an initial state of rest (Mintz, 1965). Although they were picked at random from the history tapes, the initial conditions for each experiment are appropriate to the given season. However, in every run the declination was set initially at its appropriate solstitial value. The solar calendar "dates" used for the summer and winter runs are shown in Table 1.

Table 1. Solar calendar "dates" for summer and winter control runs and experiments with 2-level UCLA model.

"Month" No.	1	2	3
Days	1-30	31-60	61-90
		Summer	
"Dates"	17 June-16 July	17 July- 15 Aug.	16 Aug. - 14 Sept.
		Winter	
"Dates"	20 Dec. - 18 Jan.	19 Jan. - 17 Feb.	18 Feb. - 19 March

A set of control runs was first carried out for both summer and winter initial conditions. In these computations a climatological mean annual sea surface temperature field was used for both seasons.[1] For all control runs, the latitude of the Northern Hemisphere snow line over the continents was specified to vary sinusoidally with calendar date, in the model used here[2], between 45°N (in January) and 75°N (in July).

In the experiment identified as NHTA (Northern Hemisphere sea surface Temperature Anomaly) a positive anomaly of 2°C to 6°C was added to the mean annual sea surface temperature over a "box" in the North Pacific Ocean between latitudes 22°N - 42°N and longitudes 140°W - 180°W. The anomaly on the perimeter gridpoints of the box was set at 2°C, increasing to 4°C at points one gridpoint in from the perimeter, and to a maximum of 6°C at points two gridpoints in from the perimeter, i.e., along 30°-34°N and 150°-170°W. This sea surface temperature (SST) anomaly pattern was suggested by the 1968 SST anomaly field in the North Pacific, as described by Namias (1971). However, it was not our purpose in this study to simulate the sequence of events discussed by Namias. The initial state of the model atmosphere does not correspond to that of the 1968 case, and even if it did, the model could not be expected to simulate with high fidelity the meteorological history observed.

The same SST anomaly was used for both the summer and winter experiments, which are designated NHTA-S and NHTA-W, respectively.

---

1 Climatological monthly mean sea surface temperatures, as well as shorter period average values, are available and have been used in other experiments. However, in all the experiments reported in this paper, we have used the mean annual sea surface temperature as the basic field.

2 A more recent version of the UCLA model permits explicit prediction of snow cover.

A third SST anomaly experiment was carried out by introducing the same positive anomaly pattern in the South Pacific Ocean, between latitudes 22°S - 42°S and longitudes 140°W- 180°W. For this experiment the initial conditions selected were those of the initial Northern Hemisphere summer (Southern Hemisphere winter) day. This experiment is designated SHTA (Southern Hemisphere sea surface Temperature Anomaly). The decision to carry out the SHTA experiment was made following the observation (discussed below) that major effects of the NHTA experiments appeared in the Southern Hemisphere after about one month, particularly in the (Northern Hemisphere) winter experiment.

The fourth experiment described in this paper was carried out to evaluate the response of the atmosphere to an anomalous snow cover. Designated SNW, the experiment consisted of shifting the mean latitude of the specified continental Northern Hemisphere snow line either 5° north or 5° south. In the former, which is designated SNW-N, the mean latitude of the snow line is placed at 65°N (rather than 60°N, as in the control cases), with a range from 50°N (in winter) to 80°N (in summer). In the latter, designated as SNW-S, the snow line varies between 40°N (in winter) and 70°N (in summer), with a mean of 55°N. Experiment SNW-S may, for example, be considered to represent a case of heavy snow early in winter (or late in the fall), which brings the snow line farther south and earlier than normal during the winter season, or a cold "late" spring, which delays the northward retreat of the snow line during the melting season. Experiment SNW-N, on the other hand, may be thought of as representing the case of a delayed beginning of winter, i.e. late arrival of the first heavy snows in middle latitudes, or perhaps a thin winter snow cover followed by rapid melting in spring and rapid northward retreat of the snow. Both experiments are admittedly somewhat unrealistic in view of the fact that there are generally significant zonal variations in both the position of the snow line over the continents and the time of occurrence of snow. However, they may give some insight into the long-term response of the atmosphere to the variable albedo and heat exchange associated with anomalies in snow cover.

The NHTA experiments

NHTA-S

The 30-day mean sea level pressure fields are shown in figures 1, 2, and 3 for the summer months 1, 2, and 3, respectively. Figures (A) show the control maps and figures (B) the anomaly maps, while figures (C) display the differences between the anomaly and control pressure fields (B - A) for each month.

In the first month the pressure differences are negligably small[1], indicating a slow response of the summer atmosphere to the SST anomaly. Small differences between the anomaly and control pressure fields begin to appear in the second month in the Northern Hemisphere, notably in the form of lower pressure on the anomaly map in the eastern Pacific. (The much larger pressure differences in the Antarctic again appear to be spurious results, the cause of which has not yet been determined.) By the third month synoptically significant differences between the mean anomaly and control pressure fields are found in both hemispheres, notably in the eastern Pacific, where a cyclone appears on the anomaly map (fig. 3-B) in place of the ridge on the control map (fig. 3-A), and in the Atlantic where an enhanced pressure gradient is found on the anomaly map between an augmented Greenland anticyclone and a deeper (than control) North Atlantic low. (A dubious pressure difference again appears in the Antarctic.)

Figure 4 (A, B, C) illustrates the 90-day time series of the regional pressure index, P, for the summer control and anomaly runs, and the difference between the two. Small effects of the SST anomaly are apparent in the east coastal pressure field after about 5 days. These effects appear to take the form mainly of phase shifts in the pressure systems rather than in wave formation or suppression. Notable exceptions are the relatively low pressure on day 31 and high

[1] The -5 mb pressure difference in the Antarctic is apparently a computational artifact, which also appears in later months.

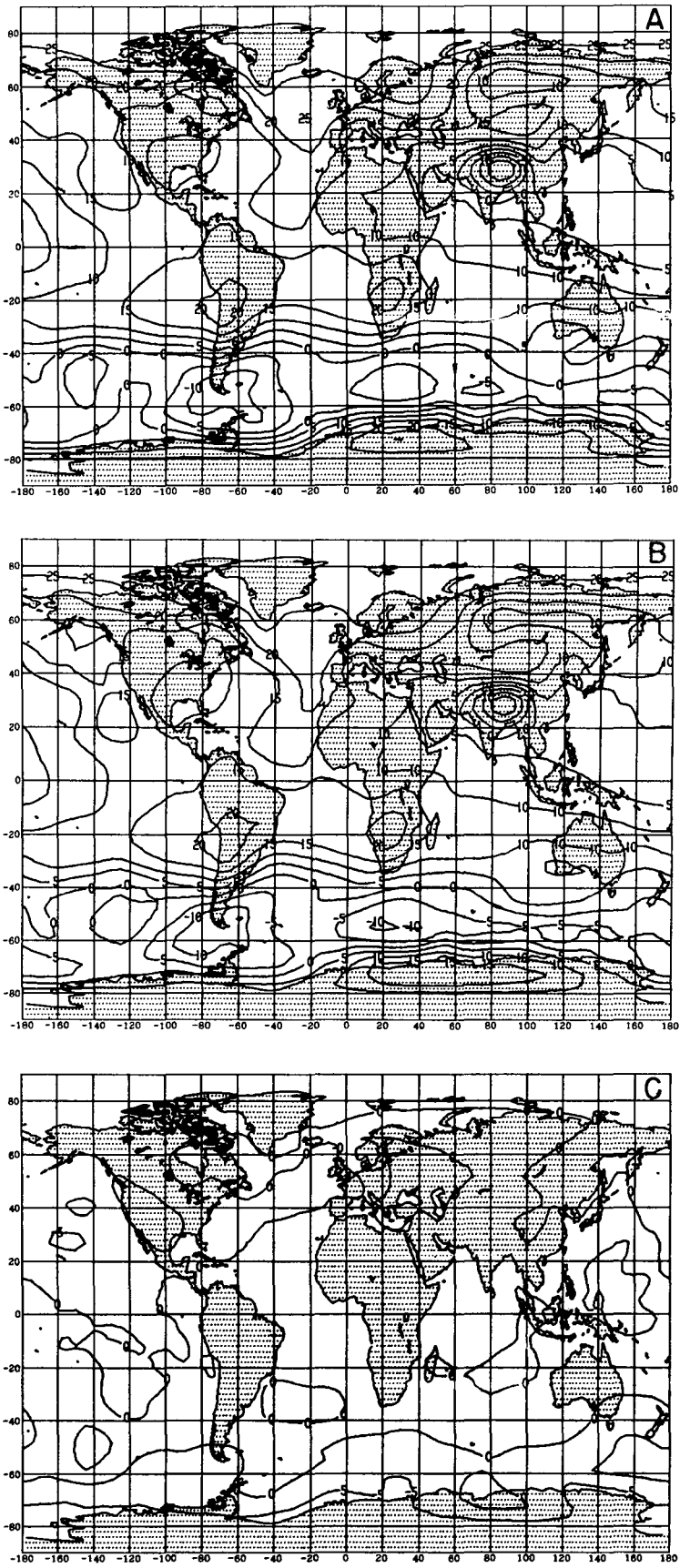

Fig. 1. Thirty-day mean sea level pressure maps for month No. 1 (1-30 days). (A) Control. (B) Anomaly. (C) Anomaly-minus-Control. Experiment NHTA-S. Isobars are labeled in millibars (mb) at intervals of ± 5 mb.

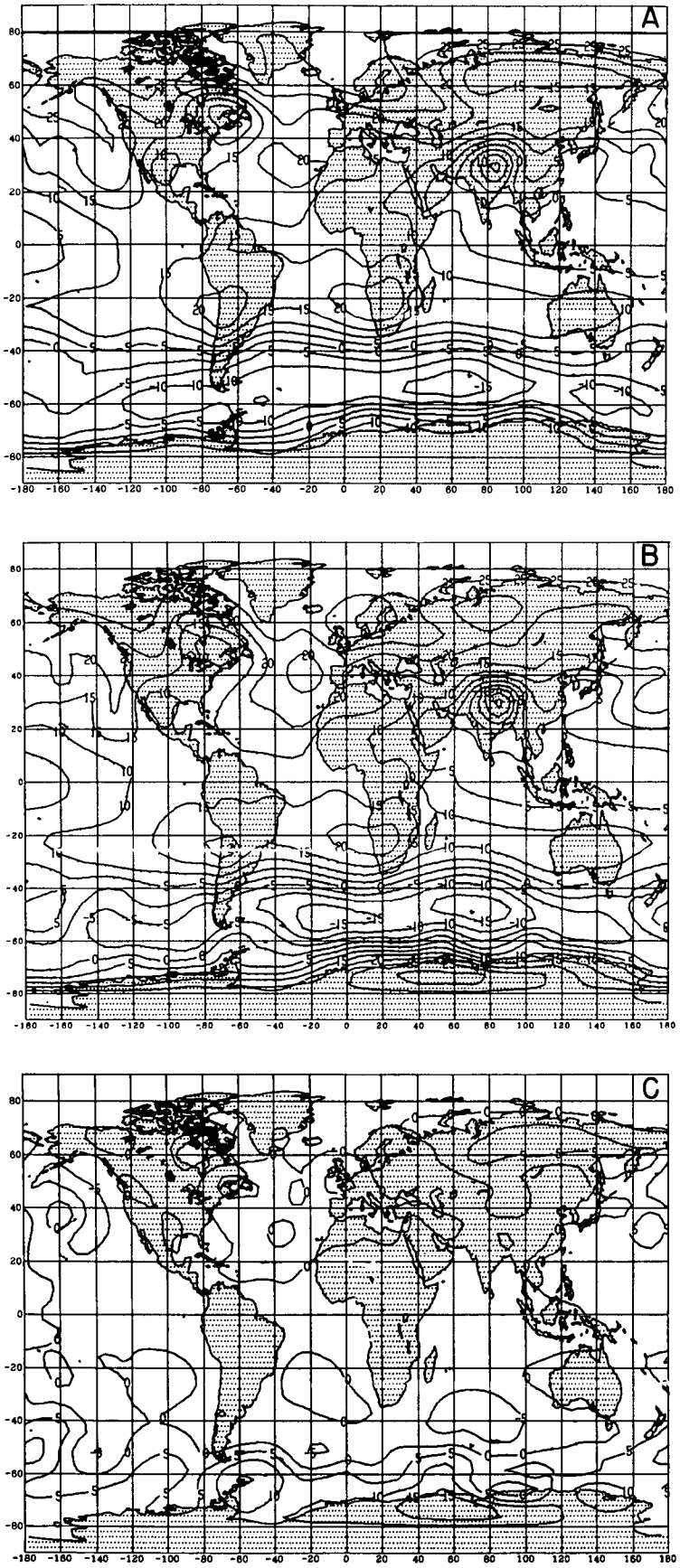

Fig. 2. Same as Fig. 1, for month No. 2 (31-60 days). NHTA-S .

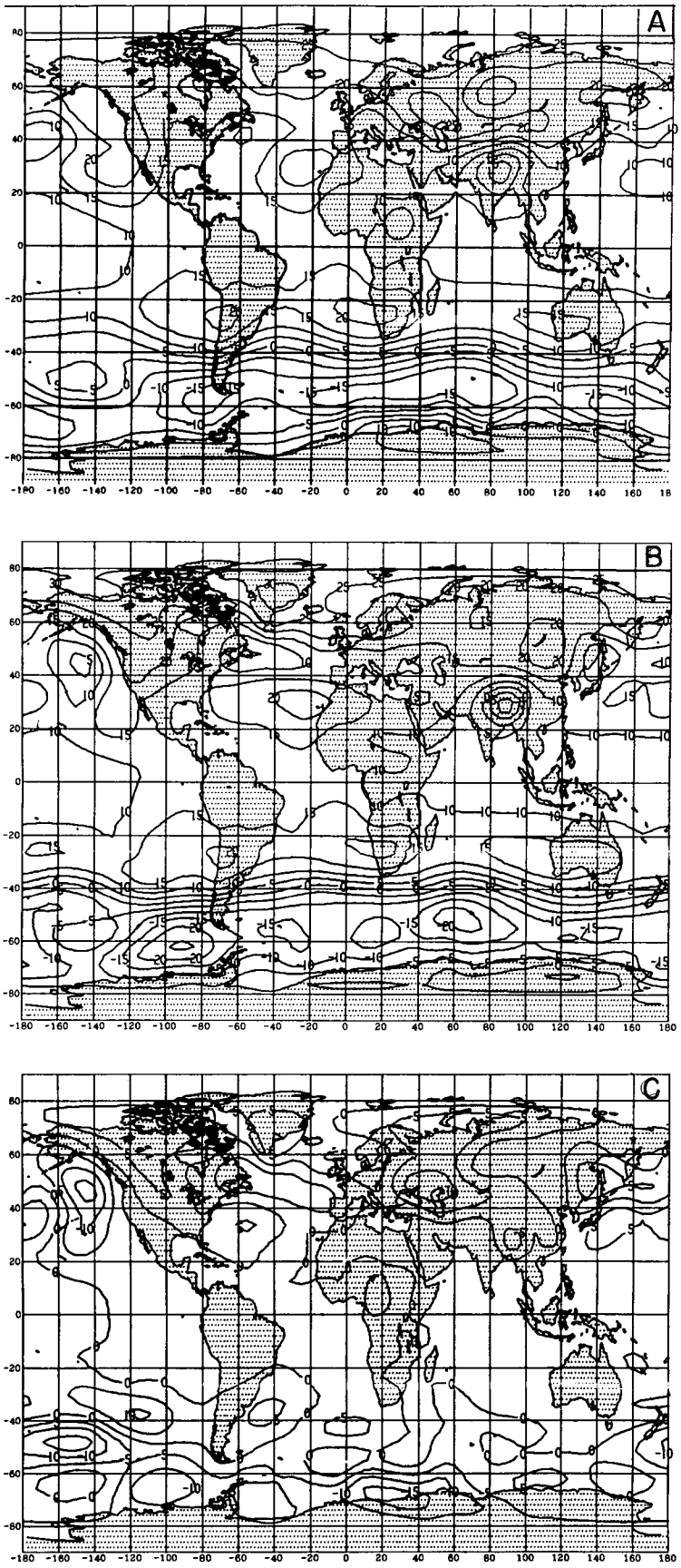

Fig. 3. Same as Fig. 1, for month No. 3 (61-90 days). NHTA-S.

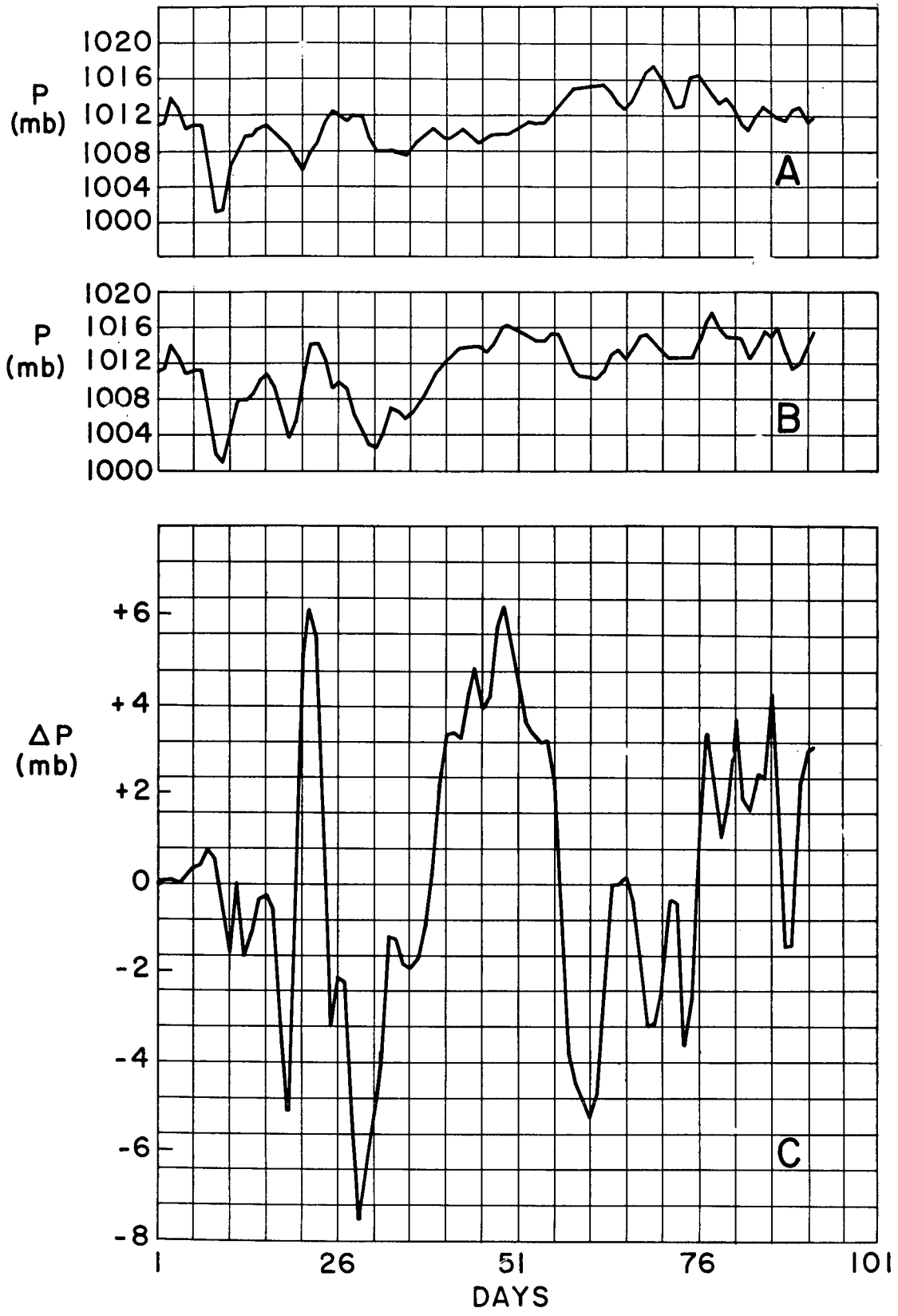

Fig. 4. Ninety-day time series of North American east coast sea level pressure index, P, in millibars, for experiment NHTA-S. (A) Control. (B) Anomaly. (C) Anomaly-minus-Control.

pressure on day 49 which appear in the anomaly series (fig. 4B) but not in the control series (fig. 4A), the differences being reflected in fig. 4C.

For each anomaly and control time series of each regional response index both Fourier spectra, for periods from 2 to 90 days, and power spectra, for periods from 2 to 20 days (based on 10 lags) were computed. A quadratic trend was computed and subtracted from each time series before the spectral analysis, and the amplitudes of the power spectra were smoothed over three cycles with a 1-2-1 smoother before plotting.

The 90-day mean values of P for the NHTA-S anomaly and control series are 1011.46 and 1011.29 mb, respectively, indicating virtually a zero overall effect of the SST anomaly on mean east coast pressures. The linear trend coefficients for the two series (plus 7.66 and 6.67 mb per 100 days, respectively) are also quite similar. (The quadratic coefficient of the anomaly series is about three times larger than that of the control series, indicating somewhat greater curvature, but the physical significance of this difference is dubious.)

The smoothed power spectra for the two P series are shown in figure 5. Here the effect of the SST anomaly appears in the form of a slight increase in variance at low frequencies (periods greater than 4 days) and a decrease in variance at higher frequencies (periods) less than 3 days). A similar shift toward the lowest frequencies in the anomaly series also appears in the Fourier spectra (not shown here).

The 90-day time series of the regional zonal index, Z, are shown in figure 6 for (A) the control run, (B) the anomaly run, and (C) the difference, anomaly-minus-control. After 6 days marked differences appear between the anomaly and control series. Principally, the SST anomaly appears to suppress large fluctuations in the Z index, and to introduce an enhanced upward trend during the latter half of the 90-day interval. Also noteworthy is the delay in the appearance of the index minimum from day 18 in the control series to day 26 in the anomaly series.

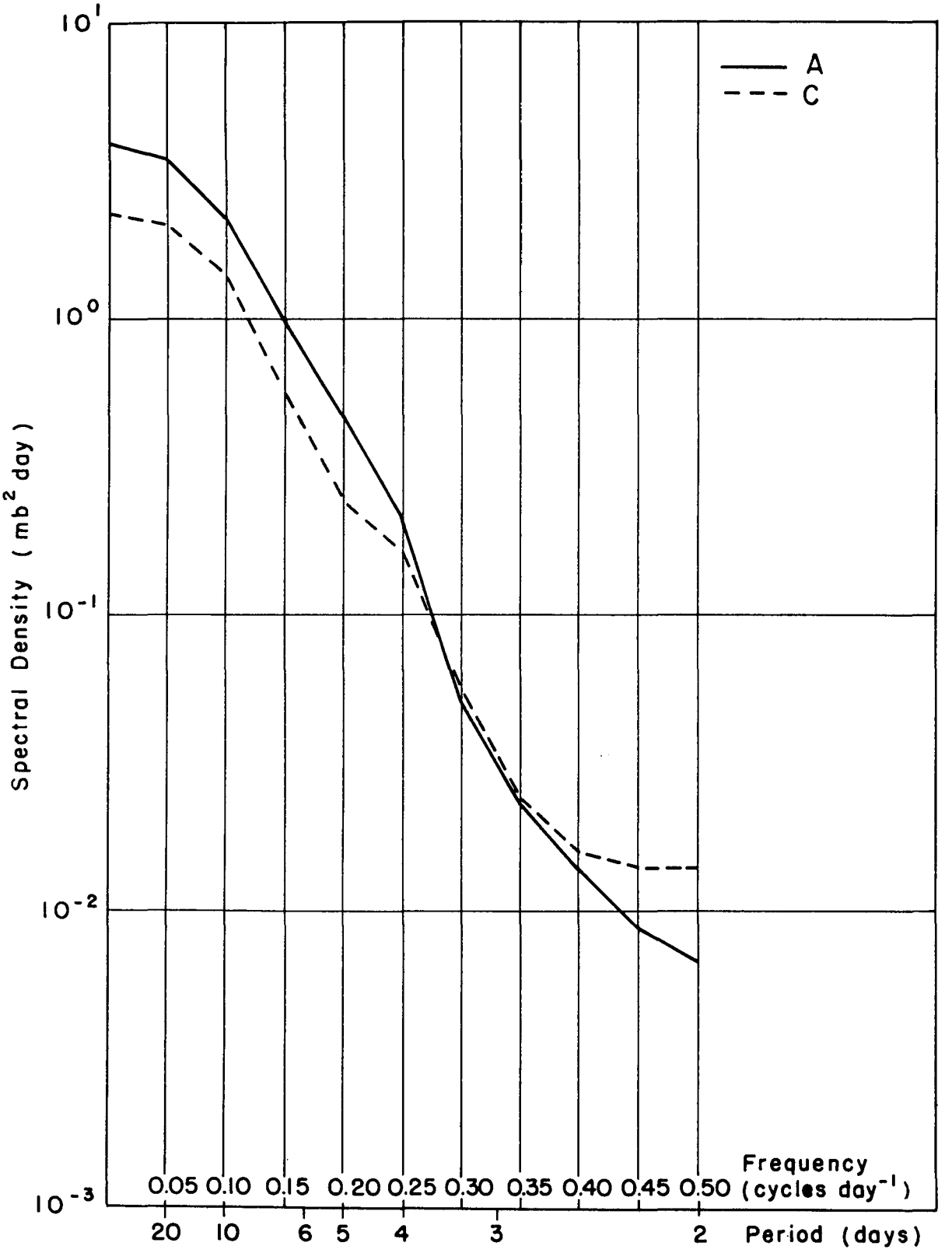

Fig. 5. Power spectra of P time series for experiment NHTA-S. A: anomaly. C: control. The quadratic trend has been removed from each series, and the spectra are smoothed over 3 cycles.

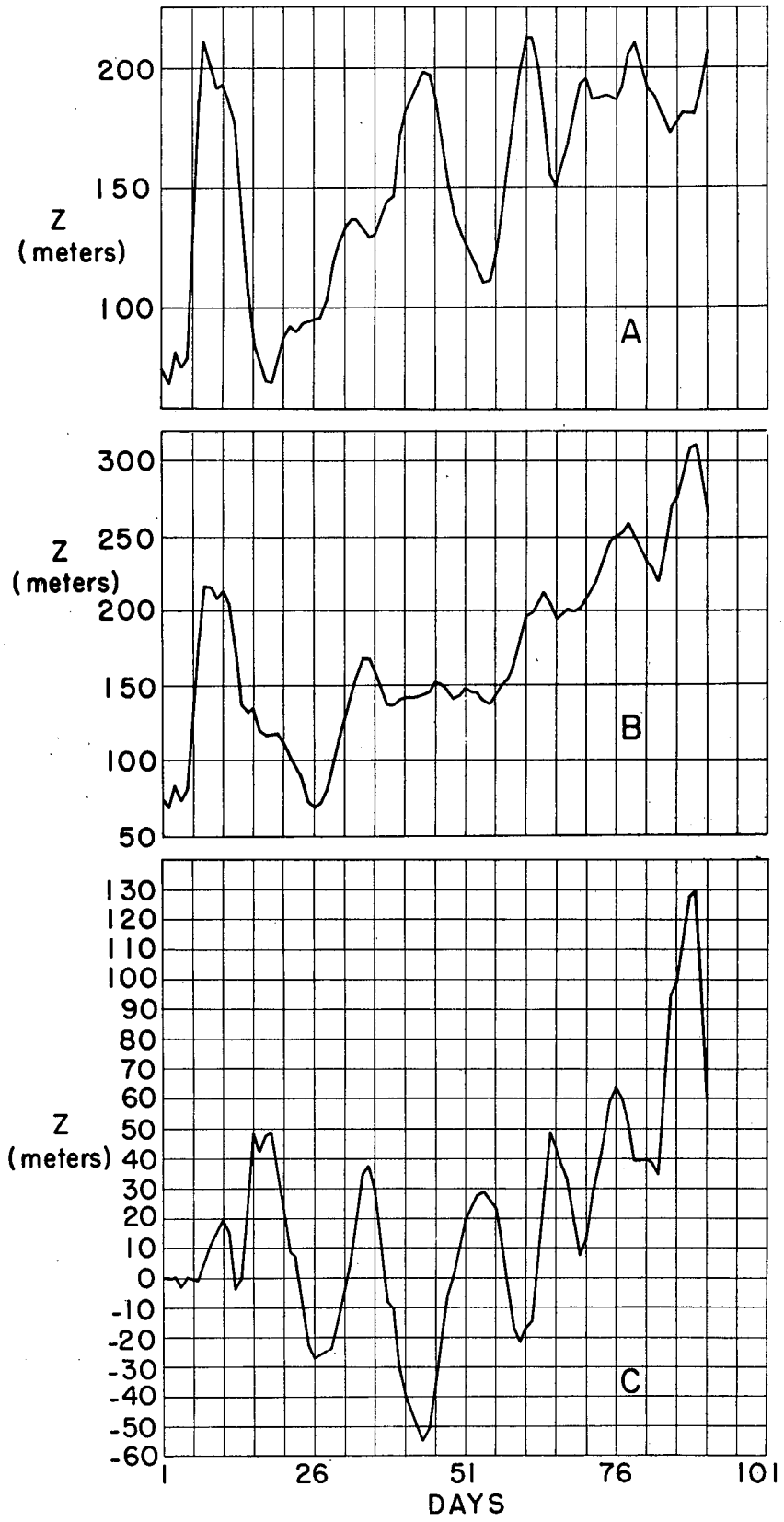

Fig. 6. Ninety-day time series of 600-mb, North American, regional zonal index, Z, in geopotential meters, for experiment NHTA-S. (A) Control. (B) Anomaly. (C) Anomaly-minus-Control.

The 90-day mean values of Z for the NHTA-S anomaly and control series are 169.7 and 151.7 meters respectively, indicating an average increase in the regional mid-latitude, mid-tropospheric westerlies due to the SST anomaly. The difference of 18 meters is equivalent to a geostrophic wind difference of only about 0.9 m sec^{-1}. This increase in the north-south slope of the 600 mb surface is consistent with the augmentation of the meridional temperature gradient between latitudes 30°N and 50°N which an SST anomaly maximum at latitude 32°N would be expected to induce. The linear trend coefficients for the anomaly and control series are -1.16 and +0.7 meters per 100 days, respectively, and are negligible for all practical purposes. This appears at first glance to be inconsistent with the augmented upward trend noted above. However, the Z curves exhibit strong curvature, so that the quadratic coefficients are relatively large while the linear coefficients are relatively small. The quadratic coefficient for the anomaly series is, in fact, an order of magnitude larger than that for the control series.

Both the power spectra and Fourier spectra of Z (neither of which are shown) exhibit an increase of high frequency variance (periods shorter than 4 days) and a slight decrease of low frequency variance (periods longer than 10 days) in the anomaly series relative to the control series. This response is unlike that found in the spectra of the P index, and its physical significance is not clear.

The 90-day time series of the North American east coastal meridional index, M, for the NHTA-S experiment are shown in figure 7 for (A) the control run, (B) the anomaly run, and (C) the difference, anomaly-minus-control. Differences are quite small for the first 15 days, after which predominantly positive differences appear, indicating either a more southerly or less northerly wind component at 600 mb in the anomaly series. The 90-day mean values of M for the anomaly and control runs are -47.2 and -72.1 meters, respectively. Thus, although both series indicate predominantly northerly winds at 600 mb, the anomaly series indicates a weaker meridional

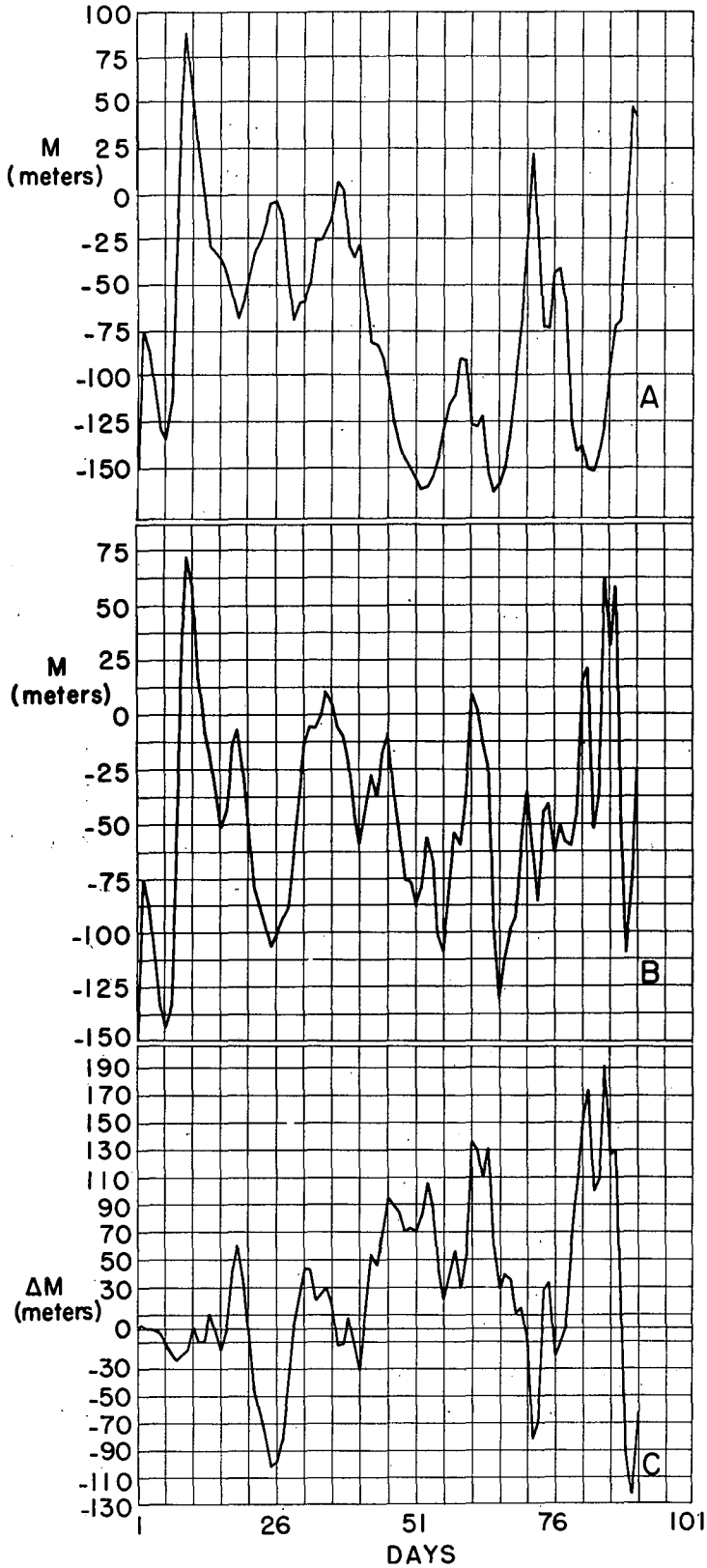

Fig. 7. Ninety-day time series of 600-mb, North American, east coastal meridional index, M, in geopotential meters, for experiment NHTA-S. (A) Control. (B) Anomaly. (C) Anomaly-minus-Control.

circulation. This is consistent with the stronger zonal circulation found in the anomaly series. The difference of 25 meters between the two mean M values corresponds to a wind difference of about 1.5 m sec^{-1}.

In summary, the NHTA-S experiment showed a relatively slow and unsystematic response of the model summer atmosphere to the Pacific SST anomaly at sea level, with large pressure effects appearing only after about 2 months. On the other hand, the SST anomaly apparently increased the north-south slope of the 600 mb surface in middle latitudes through an increase in the meridional temperature gradient, causing modest changes in the circulation indices.

NHTA-W

Because of the greater air-sea temperature contrasts in winter, as well as the stronger winds and lower stabilities found in winter over the oceans, a given positive SST anomaly may be expected to produce larger sea-to-air heat fluxes in winter than in summer, and hence a larger and faster dynamical response. As shown below, this does indeed appear to be the case in the NHTA-W experiment.

Figures 8, 9, and 10 illustrate the 30-day mean pressure fields for the control and anomaly runs, and the difference fields (anomaly-minus-control) for each month of the 90-day winter series. In the first month (Fig. 8), the cyclone in the Gulf of Alaska is seen to be deeper on the anomaly map than on the control map, while the pressure over northwestern Canada is higher on the control map. In the central North Pacific, pressures are high on the anomaly map, and the central Atlantic cyclone has been weakened relative to that on the control map. A band of lowered pressures extends across North America from the Gulf of Alaska to Labrador on the difference map (fig. 8C). Elsewhere, the pressure differences in the first month of the SST anomaly are quite small.

In the second winter month (fig. 9), the pressure differences between anomaly and control maps have virtually disappeared in the North Pacific except for a slight westward shift of the Pacific low on the anomaly

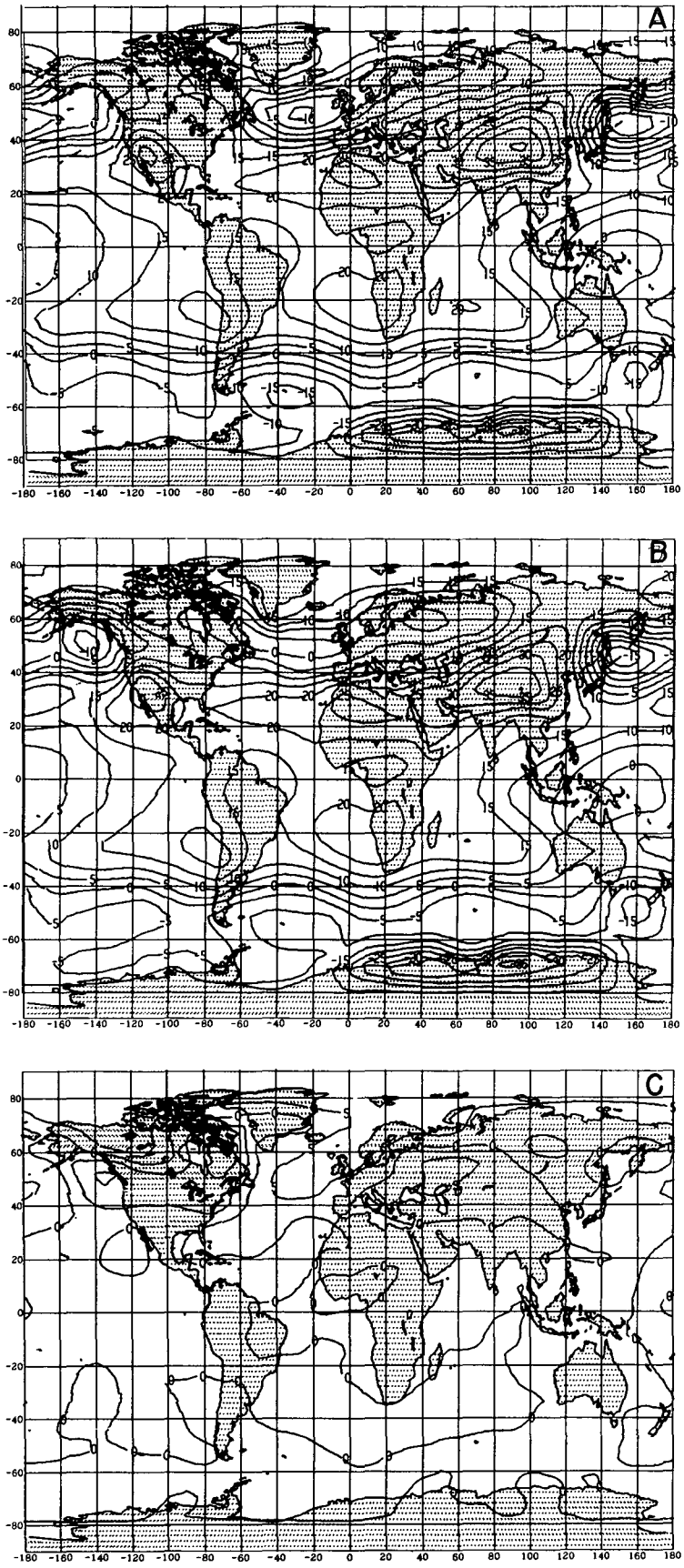

Fig. 8. Thirty-day mean sea level pressure maps for month No. 1 (1-30 days). (A) Control. (B) Anomaly. (C) Anomaly-minus-Control. Experiment: NHTA-W. Isobars are drawn at intervals of ± 5 mb.

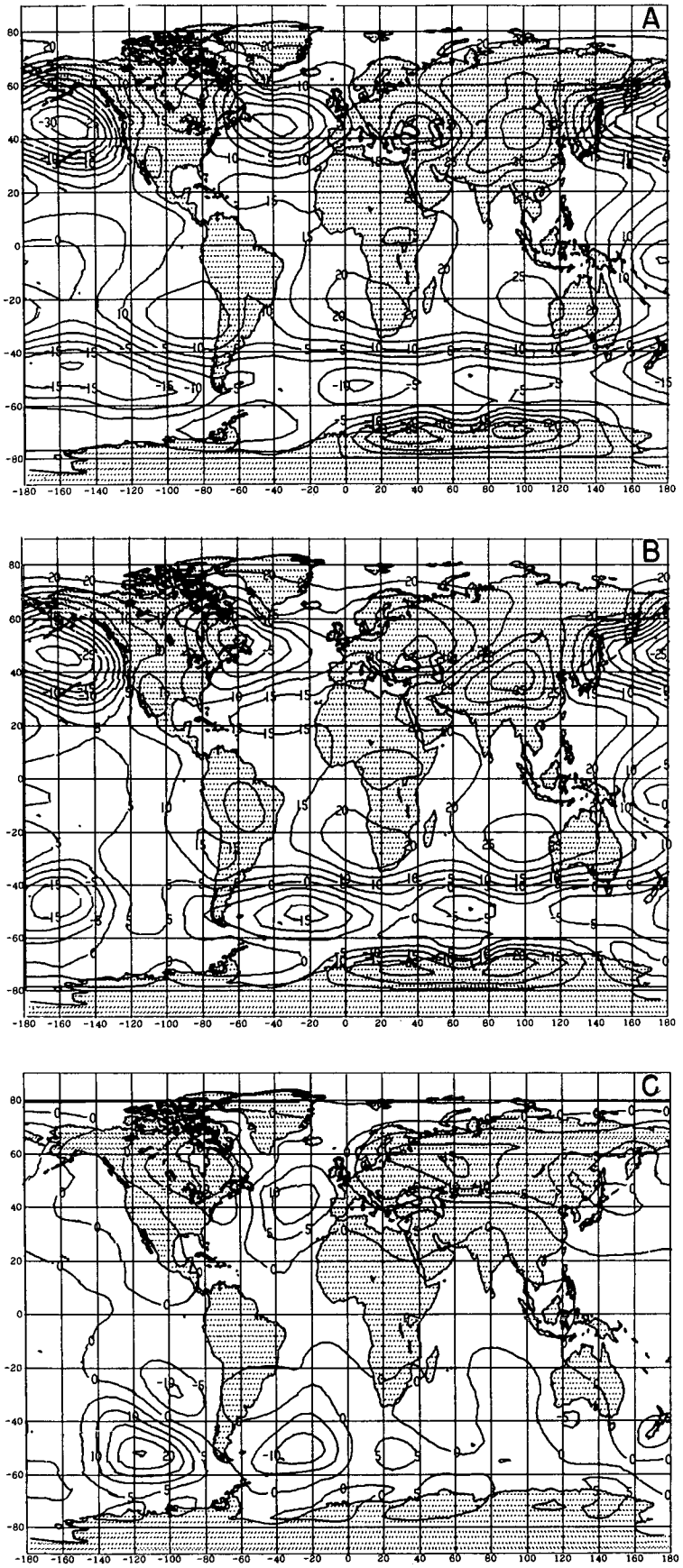

Fig. 9. Same as Fig. 8, for month No. 2 (31-60 days). NHTA-W.

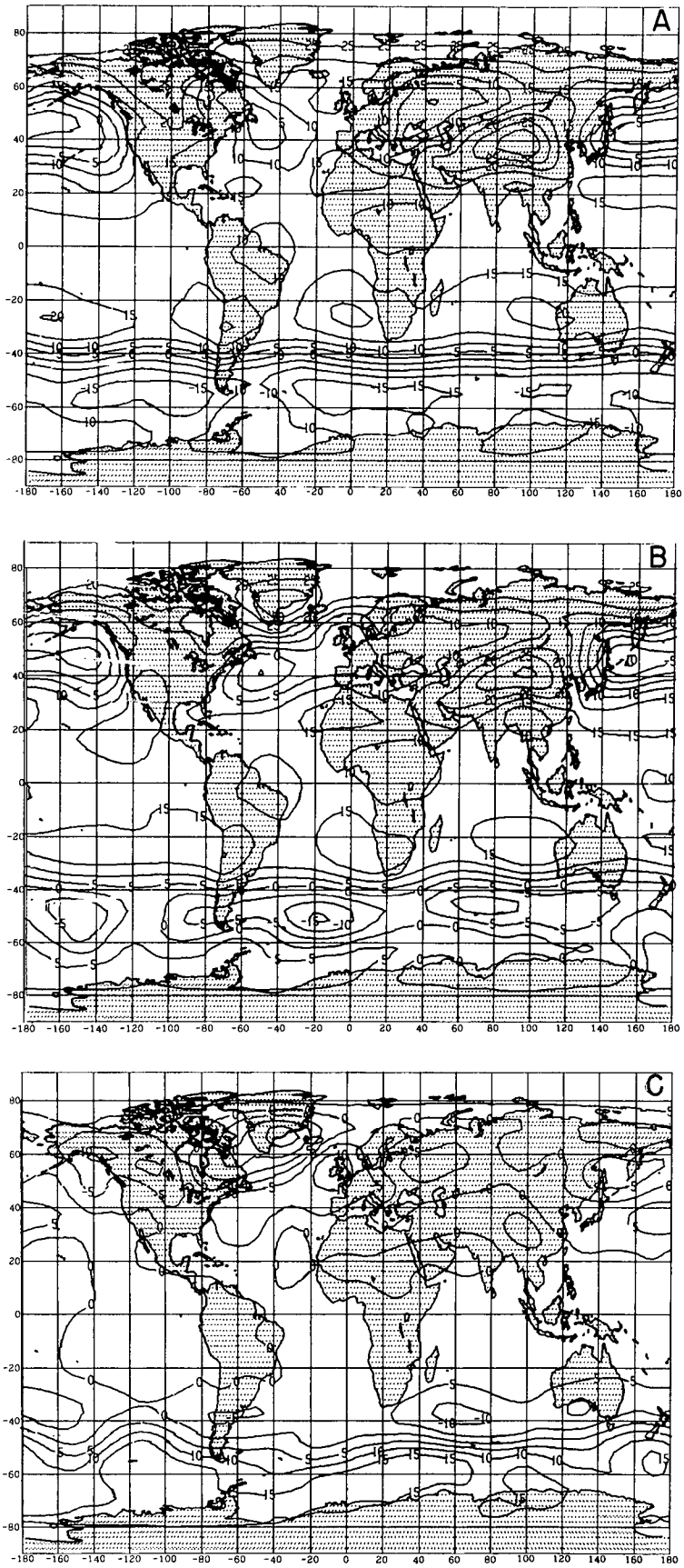

Fig. 10. Same as Fig. 8, for month No. 3 (61-90 days). NHTA-W.

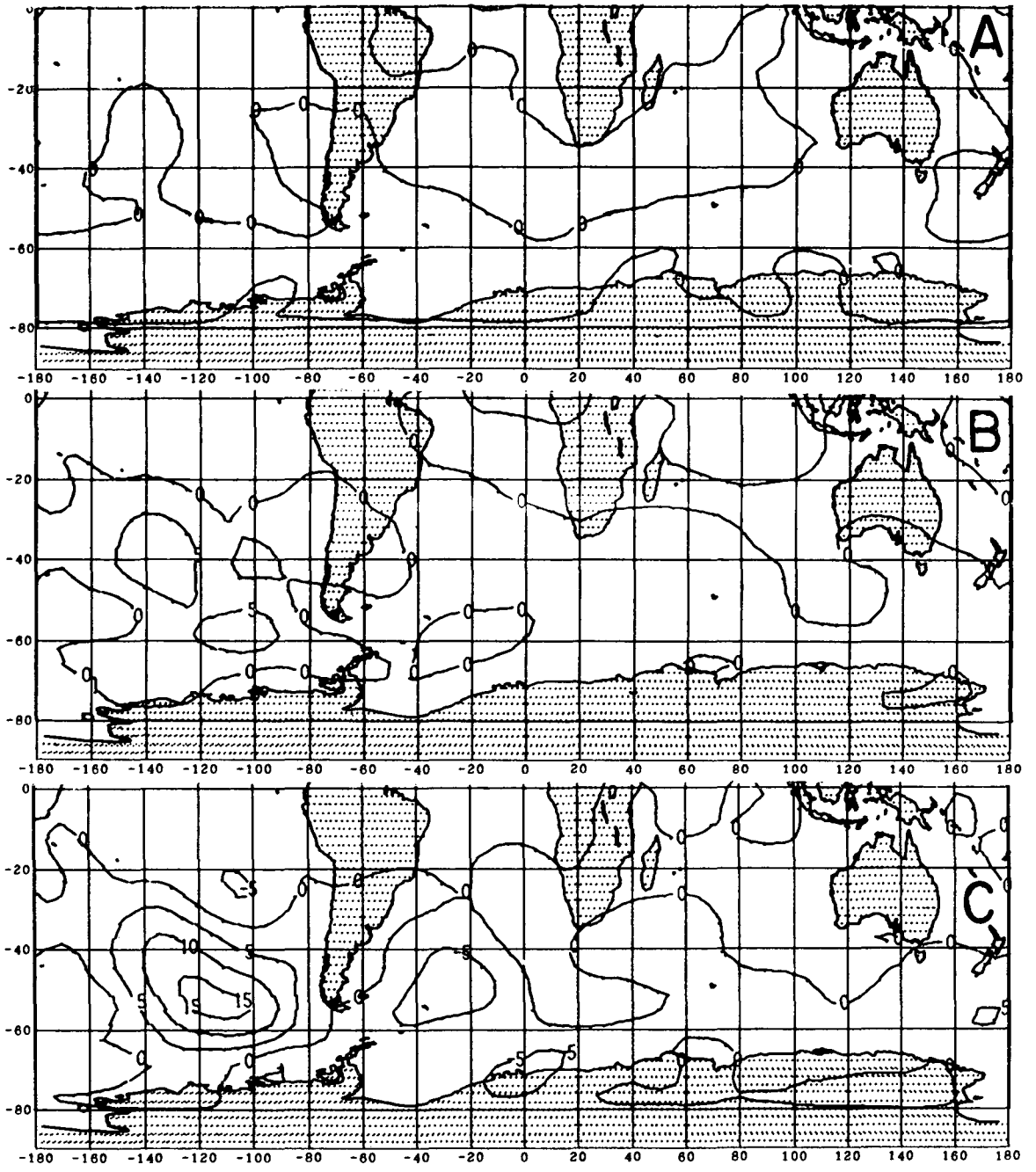

Fig. 11. Thirty-day mean anomaly-minus-control sea level pressure differences in the Southern Hemisphere in experiment NHTA-W. The maps shown are for overlapping 30-day periods stepped at an interval of 10 days. (A) 1-30, (B) 11-40, (C) 21-50, (D) 31-60, (E) 41-70, (F) 51-80, and (G) 61-90 days. Isobars are drawn at intervals of ±5 mb.

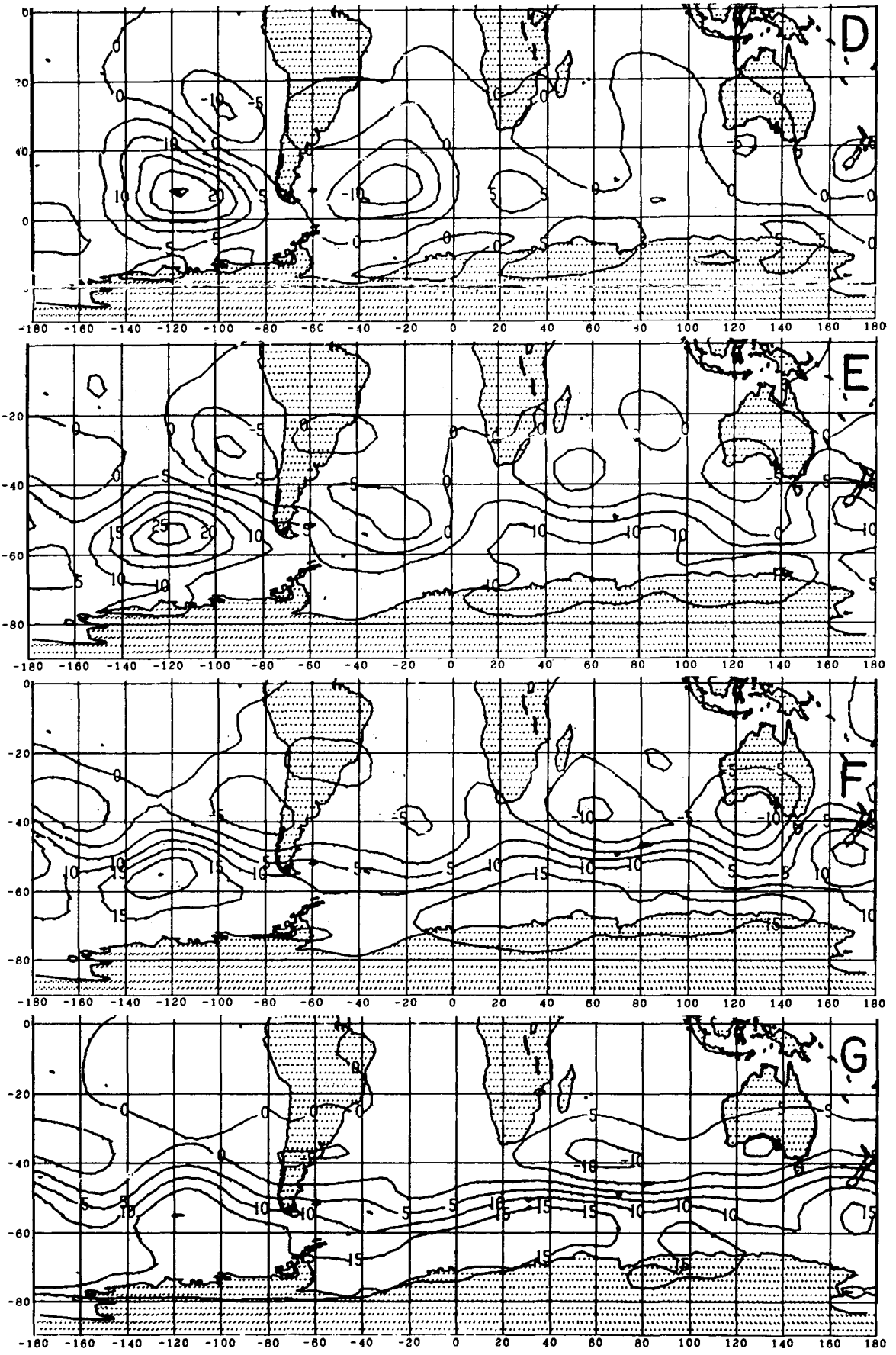
D
E
F
G

map. However, in the North Atlantic the cyclone on the anomaly map appears displaced considerably westward of its position on the control map. Pressures on the anomaly map are generally lower over Europe and Asia than on the control map. Both these features are reflected on the difference map (fig. 9-C). Perhaps the most interesting development is found in the Southern Hemisphere where the anomaly and control pressure gradients are reversed relative to each other across the southern tip of South America. This response shows up most clearly on the difference map. A similar effect, but in much weaker form, also appeared in the NHTA-S experiment (fig. 3-C) one month later.

In the third month (fig. 10) the major differences between the anomaly and control pressure fields are again found in the North Atlantic and in the Southern Hemisphere. In the North Atlantic the anomaly map exhibits a strong Greenland anticyclone and a deep Atlantic low relative to the control map, as shown by the large pressure gradient south of Greenland on the difference map (fig. 10-C). A similar response, but much less intense, was also noted in the third month of experiment NHTA-S (fig. 3-C). The effect of the North Pacific SST anomaly on the Southern Hemisphere pressure field in the third month takes the form of weaker westerlies on the anomaly map relative to the control field. With pressures on the anomaly map higher in the sub-Antarctic low pressure belt and lower in the Southern Hemisphere subtropical high pressure belt than on the control map, the meridional sea level pressure gradient in middle latitudes of the Southern Hemisphere has been significantly weakened in the third month by the SST anomaly.

The evolution of the Southern Hemisphere response to the North Pacific SST anomaly is illustrated in fig. 11. Here a sequence of seven overlapping 30-day mean anomaly-minus-control pressure difference maps, stepped at 10-day intervals, shows the appearance of a positive pressure "disturbance" in the South Pacific Ocean in the second period (11-40 days, fig. 11-B), its amplification and the negative

pressure reaction in the South Atlantic in the next two periods (21-50 and 31-60 days, figs. 11-C and 11-D), and the subsequent zonal spreading of the pressure effect toward the end of the 90-day interval. It is noteworthy that the effect of the SST anomaly on the Southern Hemisphere sea level pressure field appears to cross the Equator without producing any visible effect on the sea-level pressures in tropical latitudes. The sea-level pressure disturbance does not appear to have the character of a traveling meridional wave, but is rather more like a standing wave with a node at the Equator in the first two months, after which it propagates zonally in the Southern Hemisphere. (Further studies of inter-hemispheric propagation will be reported in a separate study.)

At this stage it is not possible to state whether the differences between the mean pressure fields described above represent physically plausible meteorological events or merely computational artifacts. Prediction experiments with various models, including the UCLA model (Charney et al., 1966), have shown how small differences in initial conditions grow with prediction time, and may lead ultimately to uncorrelated predicted states. However, the fact that the mean pressure patterns for the control and anomaly runs, even after 60-90 days, exhibit more similarities than differences (see, e.g., the North Pacific) indicates that the "noise" introduced by the SST anomalies does not destructively contaminate the global forecasts. At least it does not appear to dominate over the climatological forcing. Therefore, in the absence of contrary evidence, it may be assumed that the prescribed SST anomalies could, in nature, result in the pressure differences computed. Certainly the most interesting effect of the SST anomaly is the response in the opposite hemisphere. If this inter-hemispheric influence is real, its significance for long range forecasting is obviously great. The SHTA experiment (described below) was designed to investigate this problem.

The 90-day time series of the regional pressure index, P, for the winter experiment are shown in figure 12. The first large difference in P (-8mb) between anomaly and control occurs after 14 days. The amplitude of the P difference curve then increases with time, and a

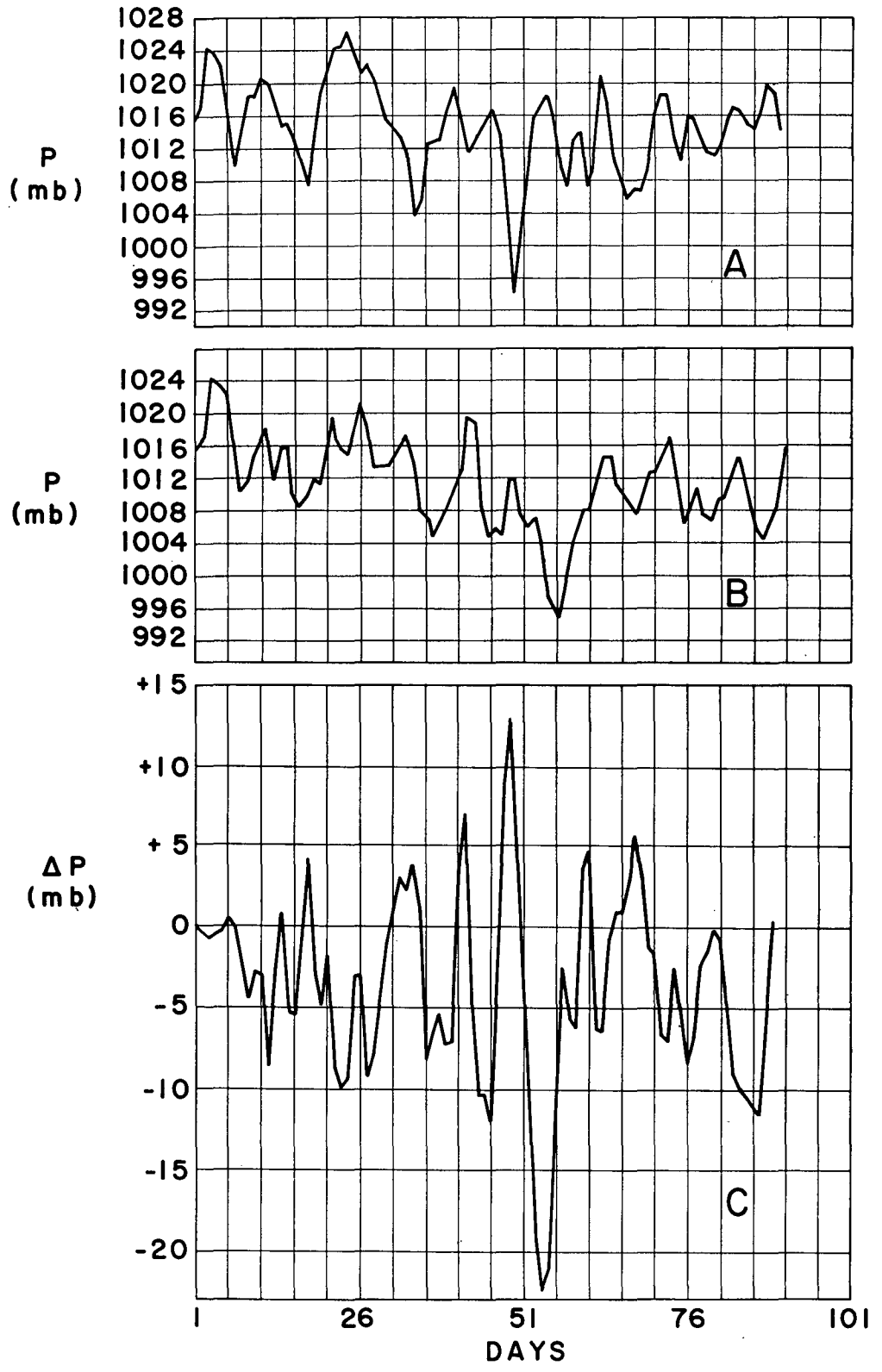

Fig. 12. Ninety-day time series of North American east coast sea level pressure index, P (mb), for experiment NHTA-W. (A) Control. (B) Anomaly. (C) Anomaly-minus-Control.

maximum difference of 13.4 mb appears on day 49. This maximum is seen to be due primarily to a phase shift in the major cyclonic event of the season on the east coast of North America. On the winter control run (fig. 12-A), P reaches a minimum of 994.22 mb on day 49, while on the anomaly run (fig. 12-B) this minimum (994.77 mb) arrives 6 days later. Thus, while the SST anomaly does not appear to generate or suppress cyclone events, it does seem to alter (in this case, retard) their phase.

The 90-day mean value of P is reduced to 1010.93 mb for the anomaly run compared with 1014.56 mb for the control run, the decrease of 3.6 mb reflecting the westward displacement of the North Atlantic cyclone which was noted in the mean maps. The linear and quadratic trend coefficients for the anomaly and control series, on the other hand, are almost identical.

Smoothed power spectra for the two P series (after removal of the quadratic trends) are illustrated in figure 13. The spectra show slightly more variance in the anomaly spectrum at the highest and lowest frequencies, with a marked reduction of variance in the intermediate frequencies (3 to 10 days). This suggests that the SST anomaly does not appear to contribute to increased sea level synoptic activity, at least in the eastern United States. Similar results are indicated by the Fourier spectra (not shown).

The 90-day time series of the Z indices for the NHTA-W experiment, shown in figure 14, indicate no clear systematic effect of the SST anomaly after a large initial increase in Z during the first month. The maximum difference of more than 220 meters between the anomaly and control Z values, which appears on day 16, may reflect the effect of an enhanced meridional temperature gradient which is probably introduced into the model atmosphere by the SST anomaly. However, this effect disappears after about a half-month. For the total 90-day period the mean values of Z are 350 and 361 meters respectively for the control and anomaly cases, the difference of only 3% representing a geostrophic wind increase of only about 0.5 $m\,sec^{-1}$. Both series

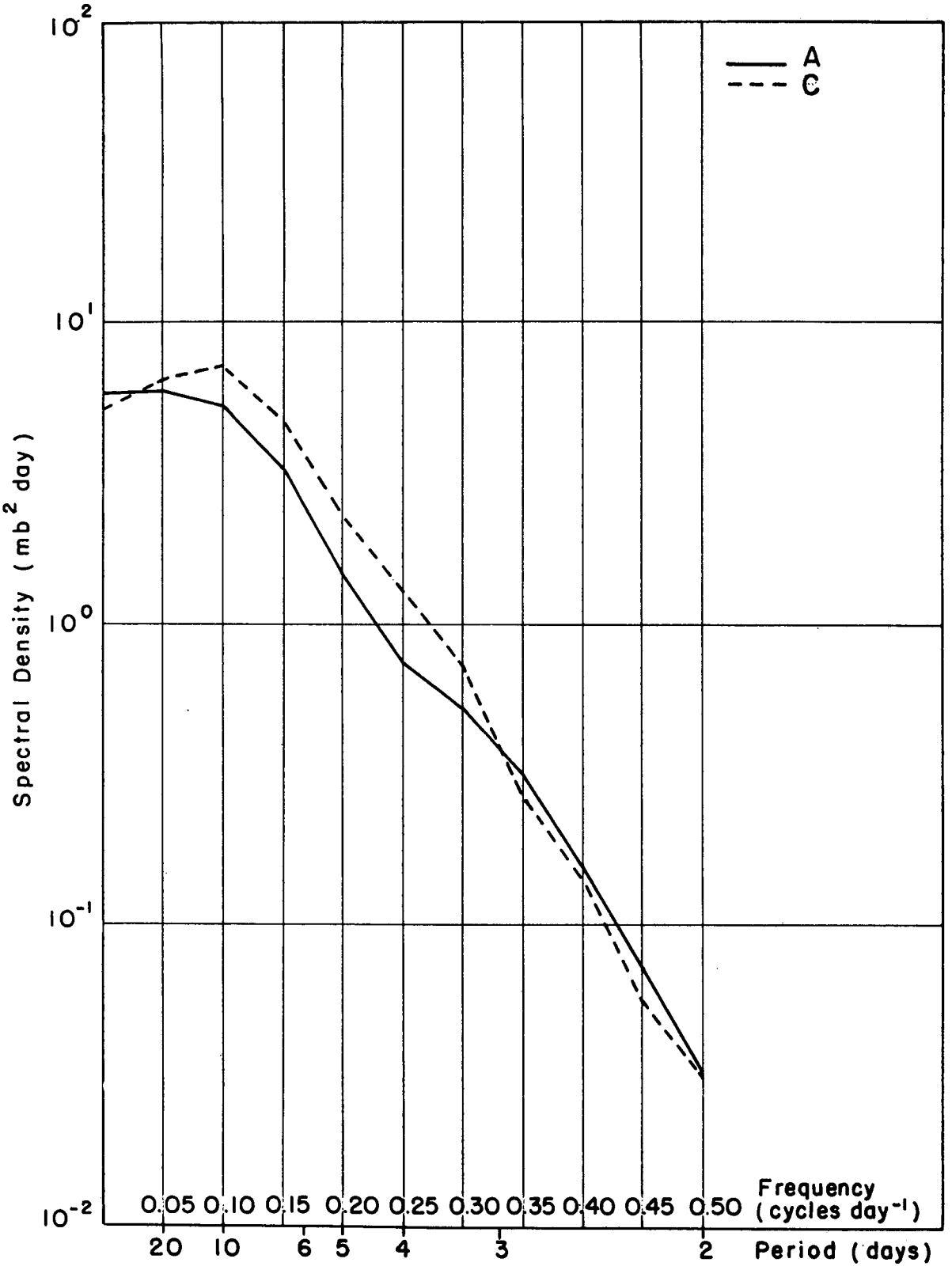

Fig. 13. Power spectra of P time series for experiment NHTA-W. A: Anomaly. C: Control. The quadratic trend has been removed from each series, and the spectra are smoothed over 3 cycles.

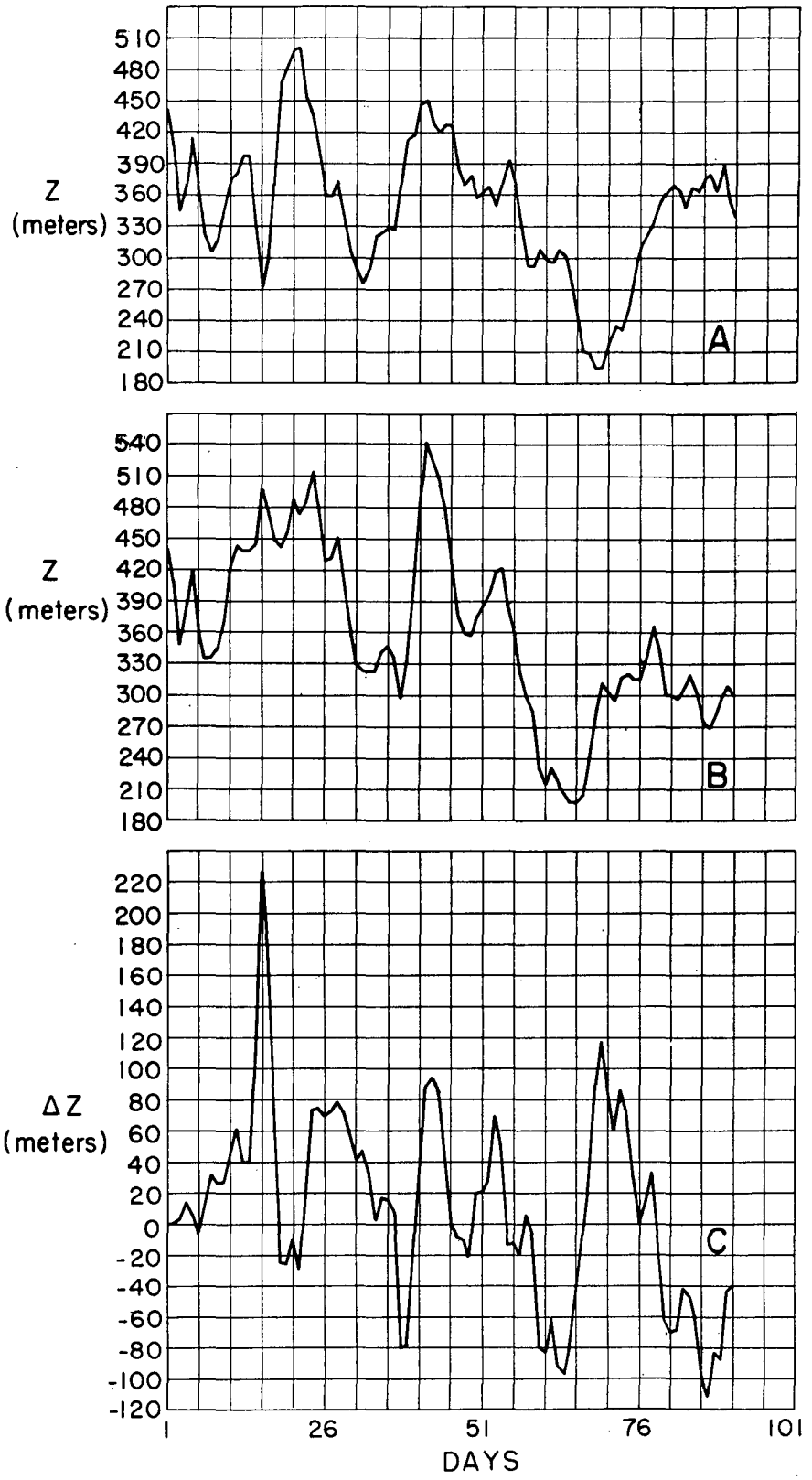

Fig. 14. Ninety-day time series of Z index for experiment NHTA-W. (A) Control. (B) Anomaly. (C) Anomaly-minus-Control. Units: geopotential meters.

exhibit small negative trends, and the spectra of the two series (not shown) are very similar, but with slightly greater variances at all frequencies in the anomaly series.

The M index time series, shown in figure 15, also fail to reveal any systematic pattern of differences between the anomaly and control runs. The 90-day mean values for the two series are almost identical, and nearly zero. The spectrum of the M index (Fig. 16), however, like that of the Z index, reveals generally greater variances in the anomaly series than in the control series over a broad range of frequencies. Thus, while the SST anomaly appears to have little effect on the variance of P, it does appear to augment the variances of the upper level circulation indices, but without any systematic alteration in this spectral distribution.

In summary, the NHTA-W experiment produced rather different results from those of the NHTA-S experiment, although some similarities between the two seasons were evident. The monthly mean sea level pressure field was modified more rapidly and more intensely especially in the North Atlantic and in the Southern Hemisphere, in the winter experiment. (A qualitatively similar response was seen in these same regions in the summer experiment.) On the other hand, the enhanced zonal index which was noted in the summer experiment appeared only as an early transient phenomenon in the winter experiment. Apparently the hydrostatic effect of an augmented meridional temperature gradient was subsequently overwhelmed by synoptic activity (presumably through energy transfers from the zonal available potential energy) in the latter case. Finally, in NHTA-W the SST anomaly appears to have contributed to a general increase in the variance of the 600 mb circulation indices, although the spectral distribution of this activity was not obviously altered.

The SHTA experiment

In this experiment the initial state of the atmosphere corresponds to 17 June, the first day of the "Northern Hemisphere Summer" period (see Table 1), and the SST anomaly is placed between latitudes

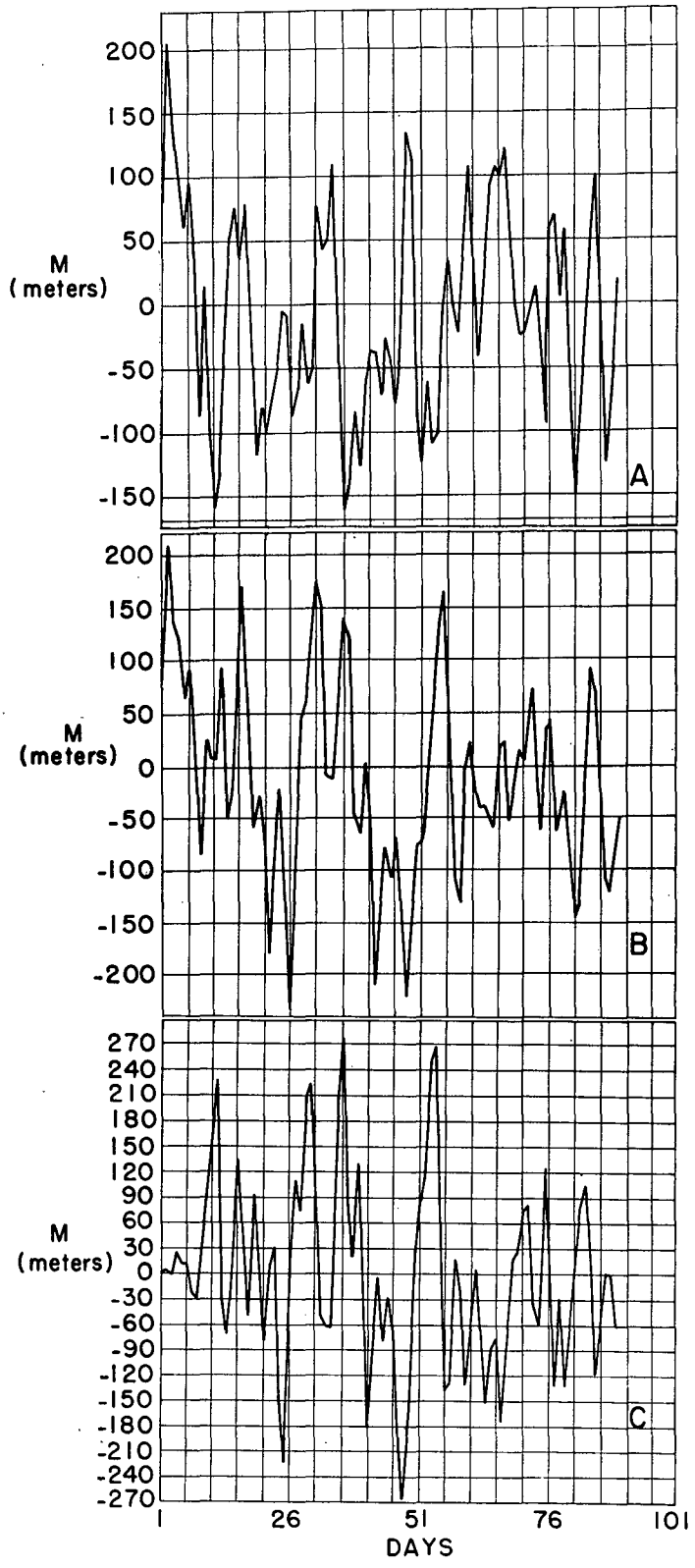

Fig. 15. Ninety-day time series of Z index for experiment NHTA-W. (A) Control. (B) Anomaly. (C) Anomaly-minus-Control. Units: geopotential meters.

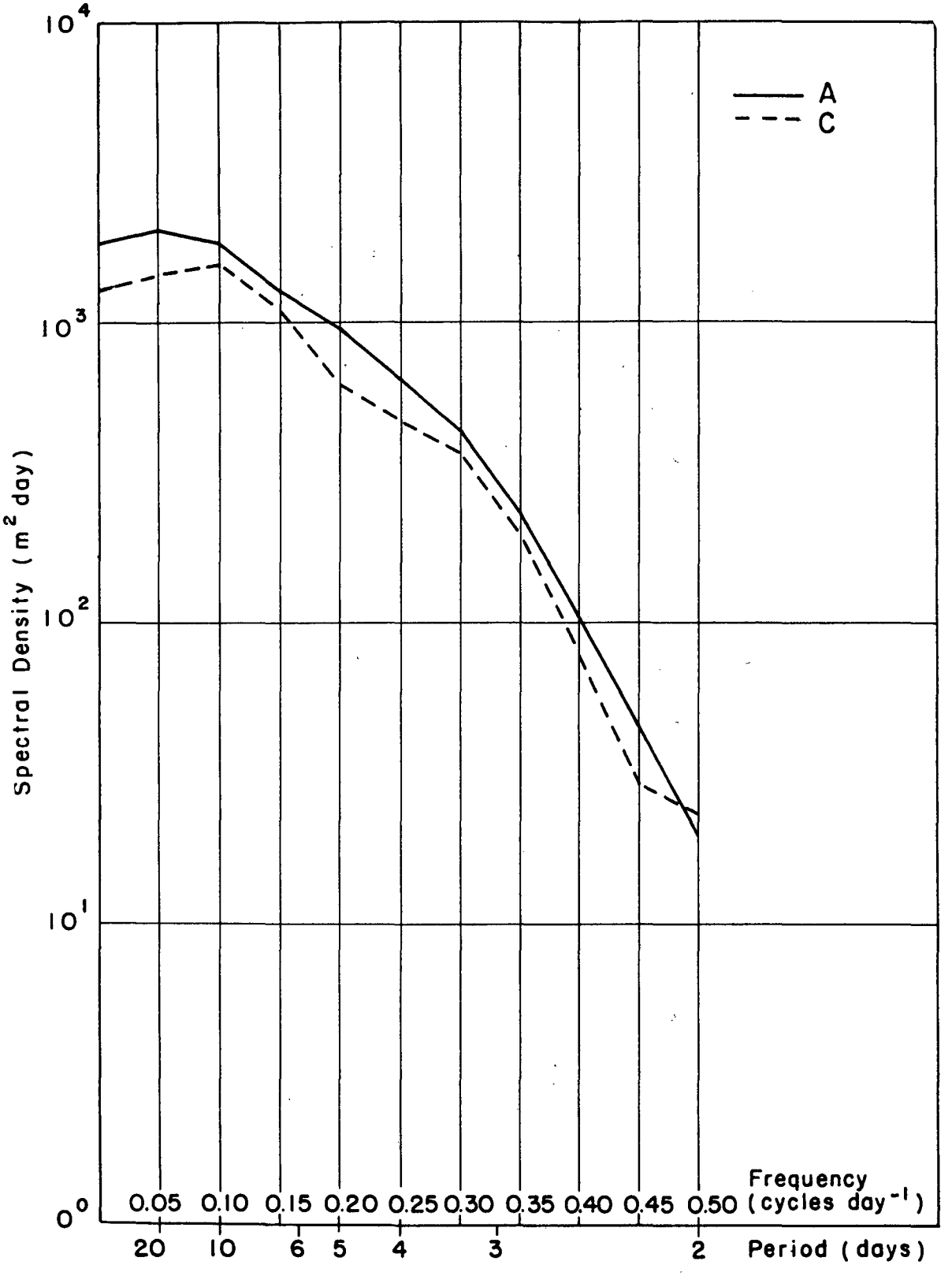

Fig. 16. Power spectra of M index time series for experiment NHTA-W. A: Anomaly. C: Control. The quadratic trend has been removed from each series, and the spectra are smoothed over 3 cycles.

22°S-42°S and longitudes 140°W-180° , in the South Pacific Ocean.

The initial dynamic response of the atmosphere to the South Pacific SST anomaly is illustrated in figure 17, which shows the computer-drawn daily sea level pressure difference maps between anomaly and control runs for days 5, 7, 9, 11, 13, and 15 in the Southern Hemisphere only. (Up to day 15 the pressure differences in the Northern Hemisphere are essentially zero.) The pressure response, as seen on these maps, has the appearance of a two-dimensional wave spreading zonally away from the SST anomaly area, but with a downwind (eastward) eccentricity, until, by day 15, the entire zonal belt from 20°S to 80°S has been "contaminated" by the SST anomaly. However, an examination of the daily printouts (not shown) of the pressure differences on the 4 degree latitude - 5 degree longitude grid for the first six days of the "forecast" reveals a more complicated response. Within the first day, the pressure at the center of the SST anomaly area falls about 5 mb below its control value. The next day this negative pressure effect shifts eastward, and on the third day it continues its eastward movement. However, as this first negative pulse leaves the SST anomaly area on the third day, it is replaced by another -5 mb pulse at the center of the area. This pulse subsequently also marches eastward. On the fourth and fifth days, positive pressure differences of 4 to 6 mb appear near the southern boundary of the SST anomaly area surrounded by a ring of falling pressures. This positive pulse moves very slowly, whereas negative pulses appear to be exported rapidly eastward from the SST anomaly area on the sixth day. Meanwhile another strong negative pressure effect reappears in the center of the area. Thus, during these first 6 days, the SST anomaly area appears to be a source of pressure pulses, continuously regenerating the synoptic sea level pressure differences in the Southern Hemisphere. The effects spread largely eastward and southward from the anomaly area, with little or no effect in the tropics during the first 6 days.

In the Northern Hemisphere small pressure differences (up to 5 mb) begin to appear after about 20 days, and by 35 days major

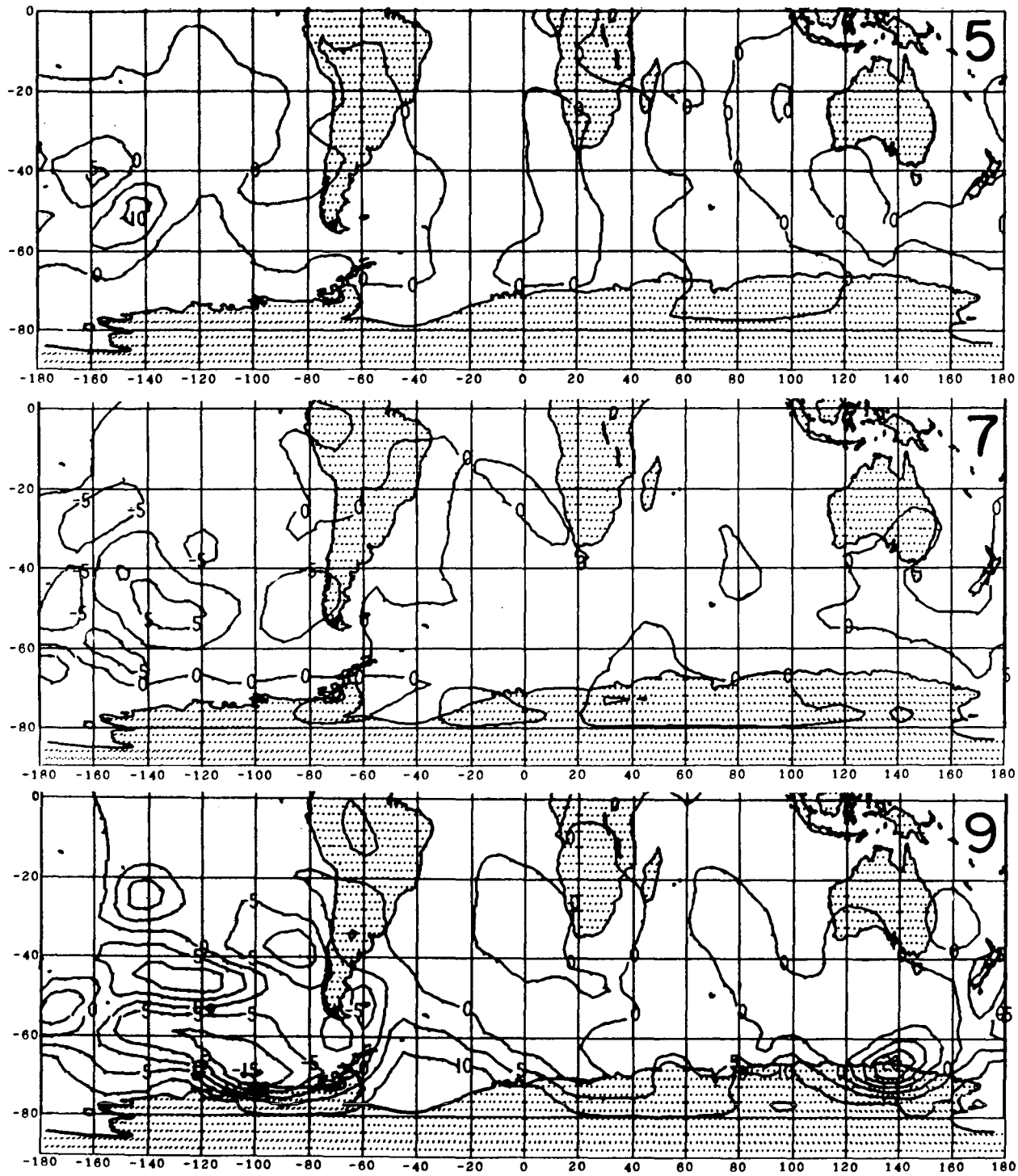

Fig. 17. Daily sea level pressure difference maps (anomaly-minus-control) for the SHTA experiment for days 5, 7, 9, 11, 13, and 15 after initial time. Isobars are drawn at intervals of ± 5 mb.

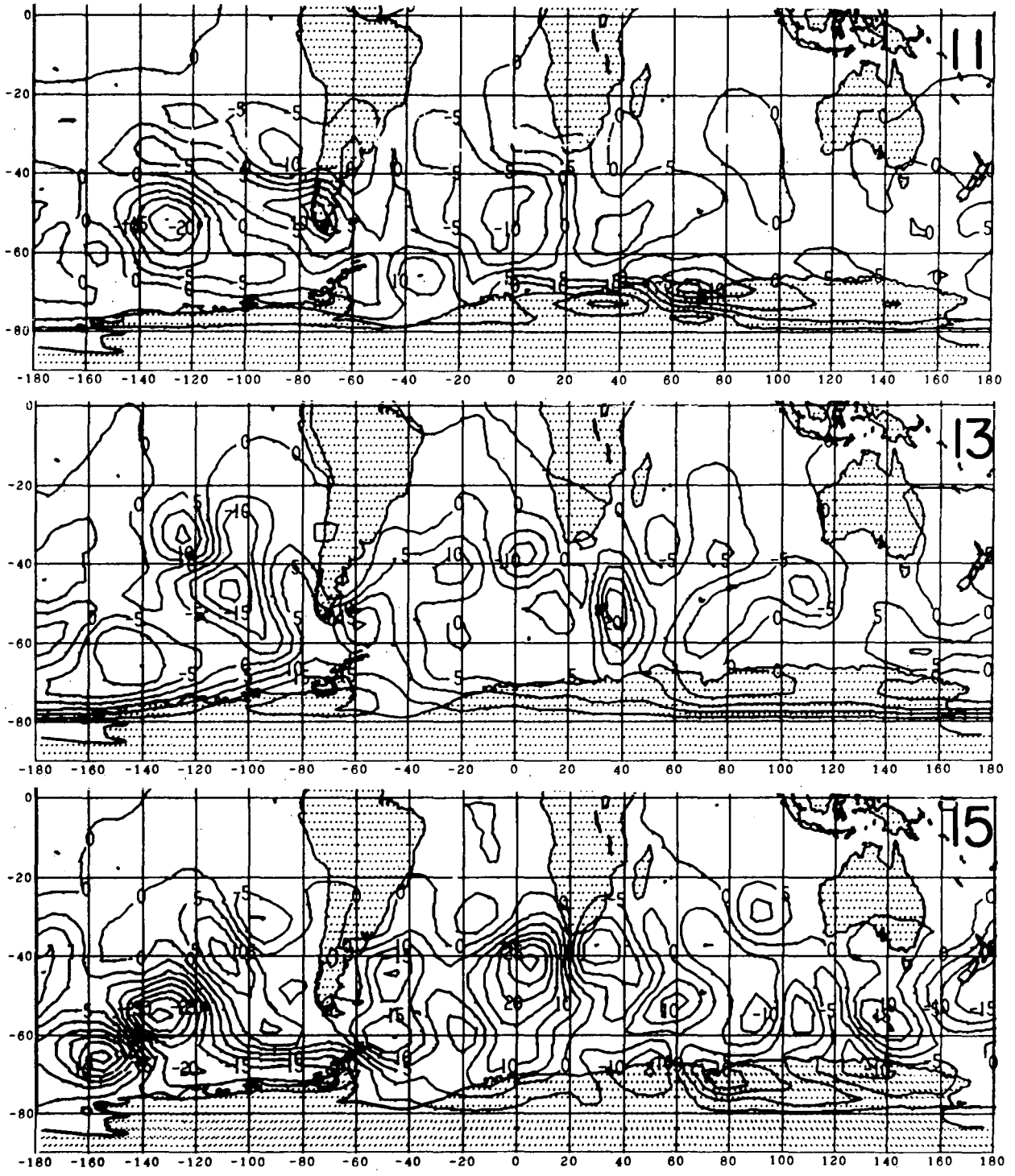
11
13
15
0
-20
-40
-60
-80
-180 -160 -140 -120 -100 -80 -60 -40 -20 0 20 40 60 80 100 120 140 160 180

pressure differences between anomaly and control are found north of the Equator. At no time in the model history, however, do the pressure differences in the equatorial region itself depart significantly from zero. The global dynamical response to the SHTA is illustrated in figure 18 in the form of (non-overlapping) 30-day mean sea level pressure difference maps. The regional response in the western half of the Northern Hemisphere is illustrated in figure 19 by overlapping 30-day mean sea level pressure difference maps, stepped at 10-day intervals.

In the Southern Hemisphere the principal long term average effect of the SHTA (see fig. 18-C) is seen to be reduced sea level pressure in the South Pacific Ocean and increased sea level pressure in the South Indian Ocean in middle latitudes (40°S-60°S).

The most prominent effect of the SHTA in the Northern Hemisphere appears in the North Atlantic region. Here, as seen in figure 19, a positive pressure change is induced after about 20 days (fig. 19-C). This effect persists through the period 51-80 days (fig. 19-F), then abruptly vanishes in the last 30 days of the 3-month period (fig. 19-G). The mean synoptic features in the North Atlantic most clearly influenced by the SHTA in the middle month are the east coastal cyclone and the Greenland high (see figure 2-A). The former is displaced from Nova Scotia to Florida and the latter is markedly intensified on the SHTA anomaly map for the period 31-60 days (not shown).

Further evidence of the Northern Hemisphere response to the SHTA can be found in the index difference time series illustrated in figure 20. All three indices (but most clearly the M index in fig. 20-C) indicate little or no reaction in the Northern Hemisphere during the first month. Subsequently the P index (fig. 20-A) exhibits differences between anomaly and control similar to those found in the NHTA-S experiment (fig. 4-C). The Z index difference (fig. 20-B) after the first month is almost consistently negative, although it does approach zero near the end of the 3-month period. This reduction in Z, presumably induced by the SHTA, is consistent with the marked increase

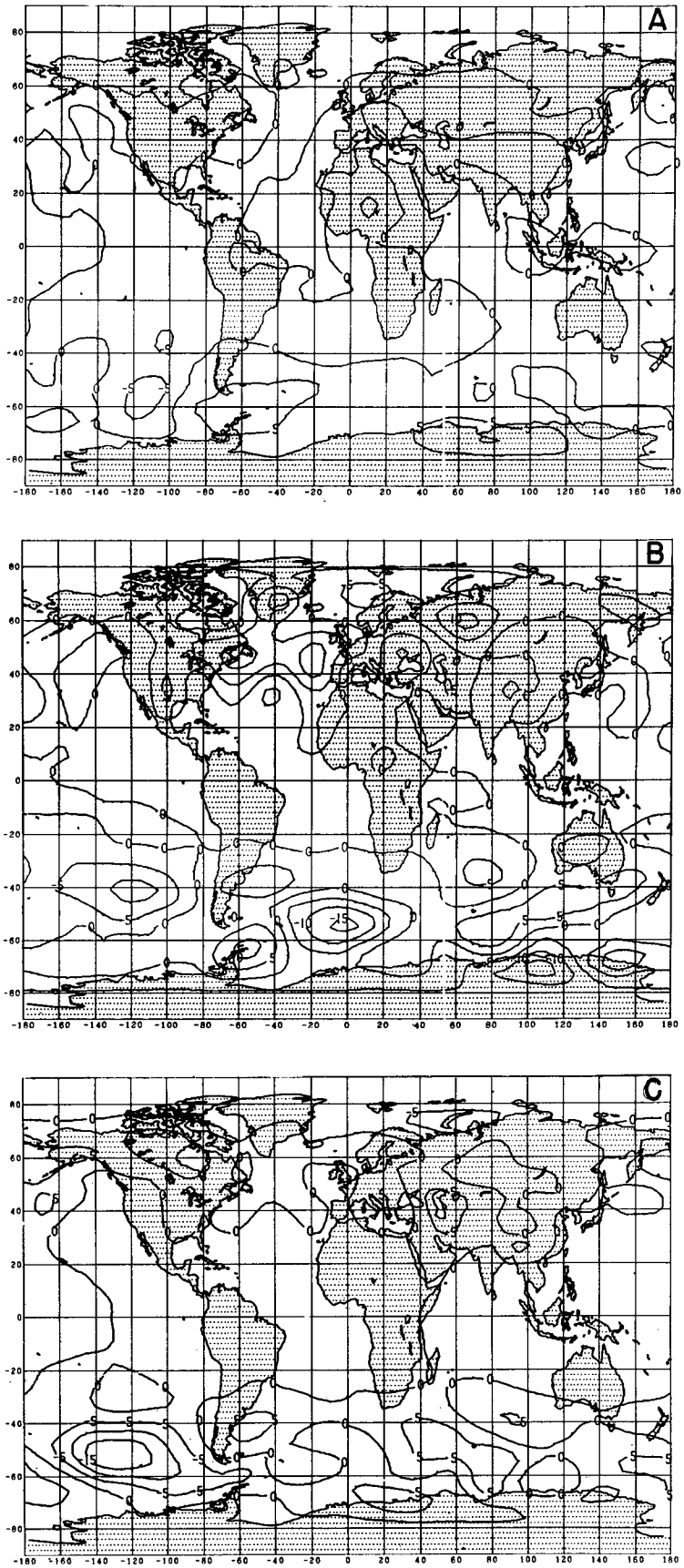

Fig. 18. Thirty-day global mean sea level pressure difference maps (anomaly-minus-control) for SHTA experiment. (A) Month #1 (1-30 days), (B) Month #2 (31-60 days), and (C) Month #3 (61-90 days). Isobars are drawn at intervals of ±5 mb.

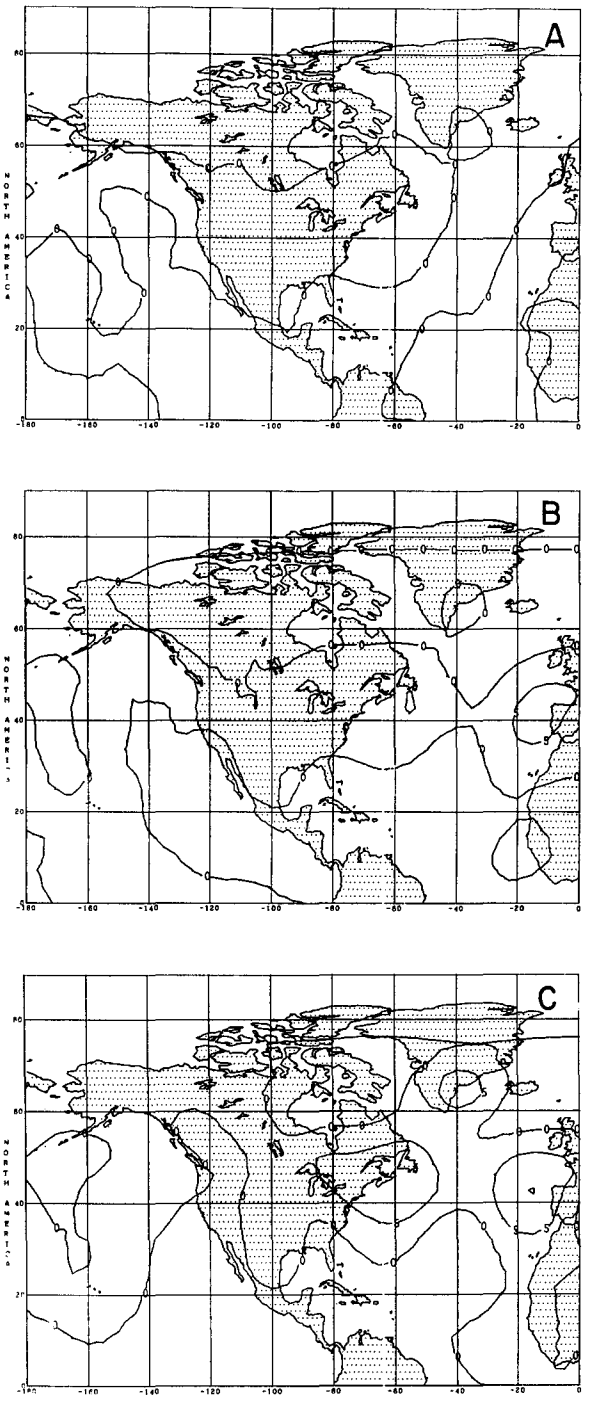

Fig. 19. Overlapping regional 30-day mean sea level pressure difference maps (anomaly-minus-control) at 10-day intervals for SHTA experiment, western half of Northern Hemisphere. (A) 1-30, (B) 11-40, (C) 21-50, (D) 31-60, (E) 41-70, (F) 51-80, and (G) 61-90 days. Isobars are drawn at intervals of ±5 mb.

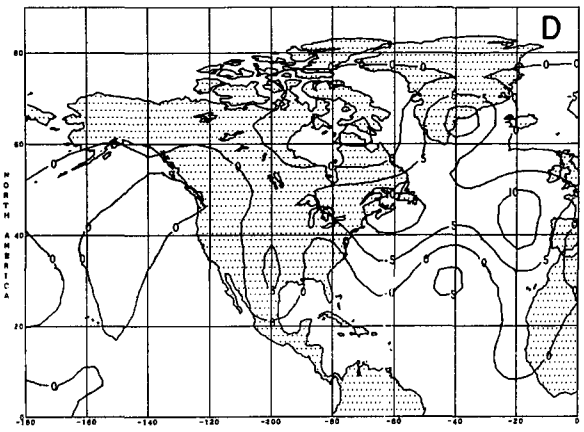
D
NORTH AMERICA

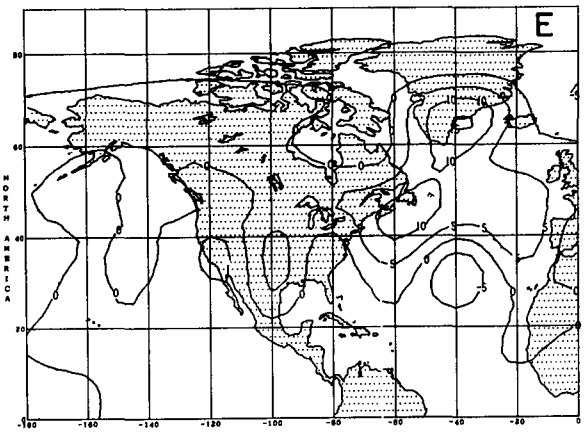
E
NORTH AMERICA

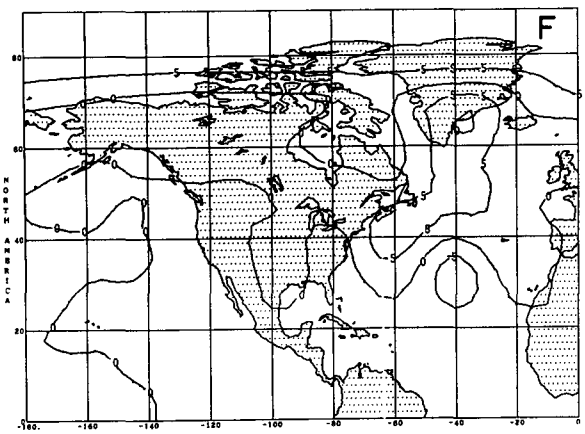
F
NORTH AMERICA

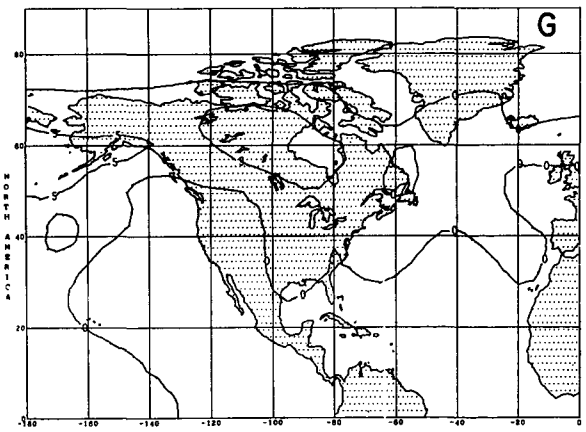
G
NORTH AMERICA

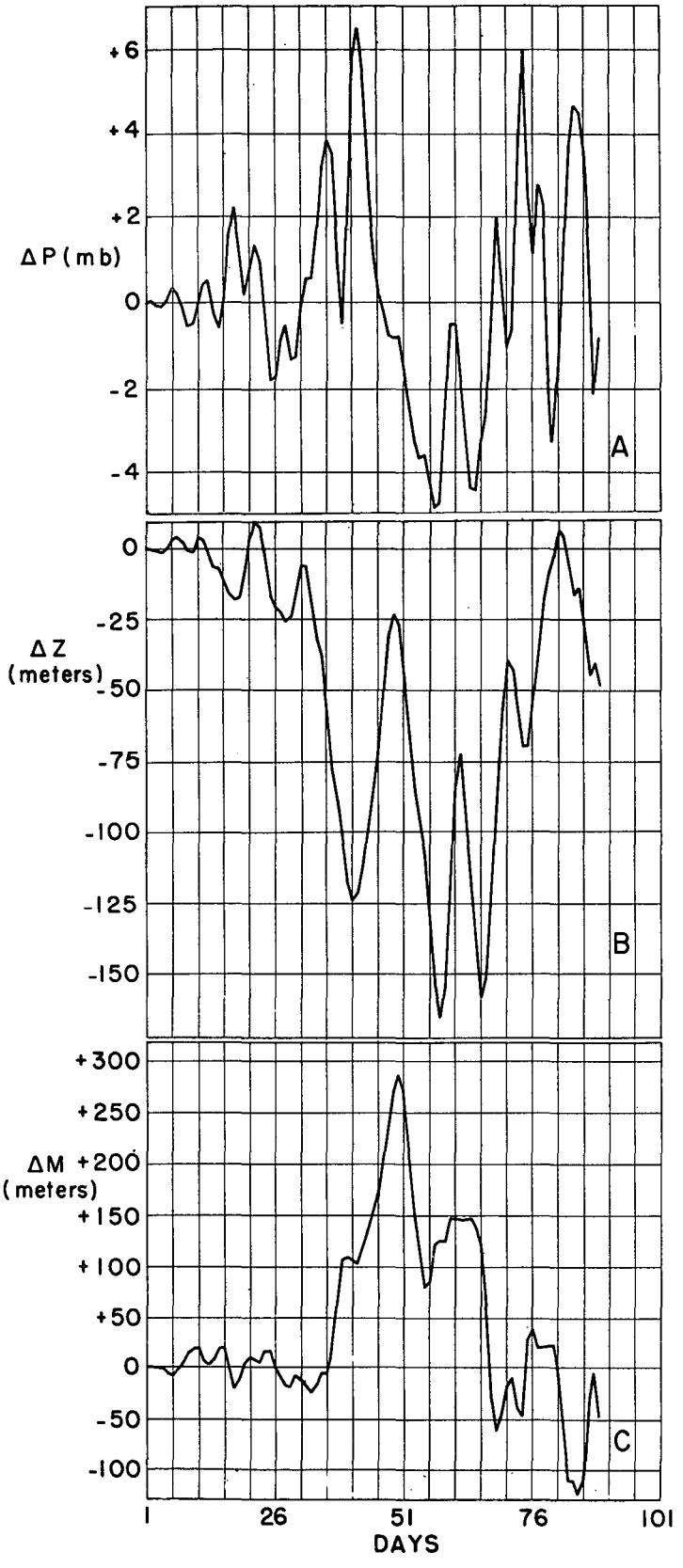

Fig. 20. Time series of differences between Northern Hemisphere regional indices (anomaly-minus-control) for SHTA experiment. (A) P index (mb), (B) Z index (geopotential meters), (C) M index (geopotential meters).

in the east coast meridional index, M (fig. 20-C) seen in the same middle period. The latter two figures taken together suggest that the effect is in the form of long wave amplification at 600 mb, and not simply a phase shift.

In summary, the interhemispheric effect of the South Pacific SST anomaly on the sea level pressure field is not simply a mirror image of that induced by the North Pacific anomaly. This is clear from a comparison of figure 18-B with figure 11-D, and of figure 18-C with figure 11-G. The interhemispheric effect in the SHTA experiment is not only synoptically different from that of the NHTA-W experiment, but is also much weaker and less persistent. Whether this is due to the different initial conditions in the two hemispheres, or to differences in land-sea distribution or ocean temperatures is not known. Nor is it clear how the South Pacific anomaly caused the 600 mb circulation indices in the western portion of the Northern Hemisphere to be altered for a period of about a month beginning one month after introduction of the anomaly. What does appear clear is that transequatorial influences propagate in the model without visibly affecting the sea level pressure field in the equatorial region or indeed anywhere in the tropics. (The manner in which influences propagate across the equator in global models will be the subject of a separate study.)

The SNW experiments

The experiments with the Northern Hemisphere continental snow line were performed only for the winter season. Thus, in the SNW-N experiment the anomaly run represents a case with the snow line at a minimum latitude of 50°N, compared with the control minimum latitude of 45°N, while the anomaly run in the SNW-S experiment corresponds to a minimum latitude of the snow line at 40°N.

In both SNW experiments the most interesting effects on the 30-day mean sea level pressure field appear in the North Atlantic region, and reflect the influence of the snow line on the

monsoonal pressure differences between the continents and the oceans in winter. The global anomaly-minus-control mean pressure difference fields are shown in figures 21 and 22 for the SNW-N and SNW-S experiments respectively for the three non-overlapping 30-day periods. Although the mean anomaly and control[1] pressure fields themselves are not reproduced here, they will be referred to in the following descriptions of the pressure response.

In the first months (Figs. 21-A and 22-A), the northward shift of the snow line (Figs. 21A) is accompanied by a northward shift of the Atlantic-European trough and a weakening of the North Atlantic cyclone, whereas the southward shift of the snow line (Figs. 22-A) produces little or no effect. The difference between SNW-N and SNW-S is, however, much more apparent in the second month. In the former case (Fig. 21-B), the large positive difference in the North Atlantic between SNW-N and the control corresponds to an almost complete disappearance of the North Atlantic low,[2] while in the latter case (Fig. 22-B) both the North Atlantic and North Pacific cyclones in SNW-S are deeper than those on the control map.[2] Thus, as might have been expected, the southward shift of the snow line appears to enhance the winter monsoonal pressure difference between the oceans and continents, while the northward shift tends to weaken it. However, although the increase in the monsoonal pressure difference associated with SNW-S persists into the third month (Fig. 22-C), the opposite effect is not found in SNW-N. Instead, the North Atlantic cyclone is restored in the third month in the latter case (Fig. 21-C), and is even intensified relative to the control, as can be seen from the large negative pressure differences in the North Atlantic. This "springing back" of the land-sea pressure difference is rather surprising, and is not readily explained. Nevertheless, it is noteworthy that the monsoonal pressure difference between land and sea in the third month

---

[1] The winter control pressure fields are, of course, shown in figures 8-A, 9-A, and 10-A.

[2] The winter control pressure field for the second month can be seen in figure 9-A.

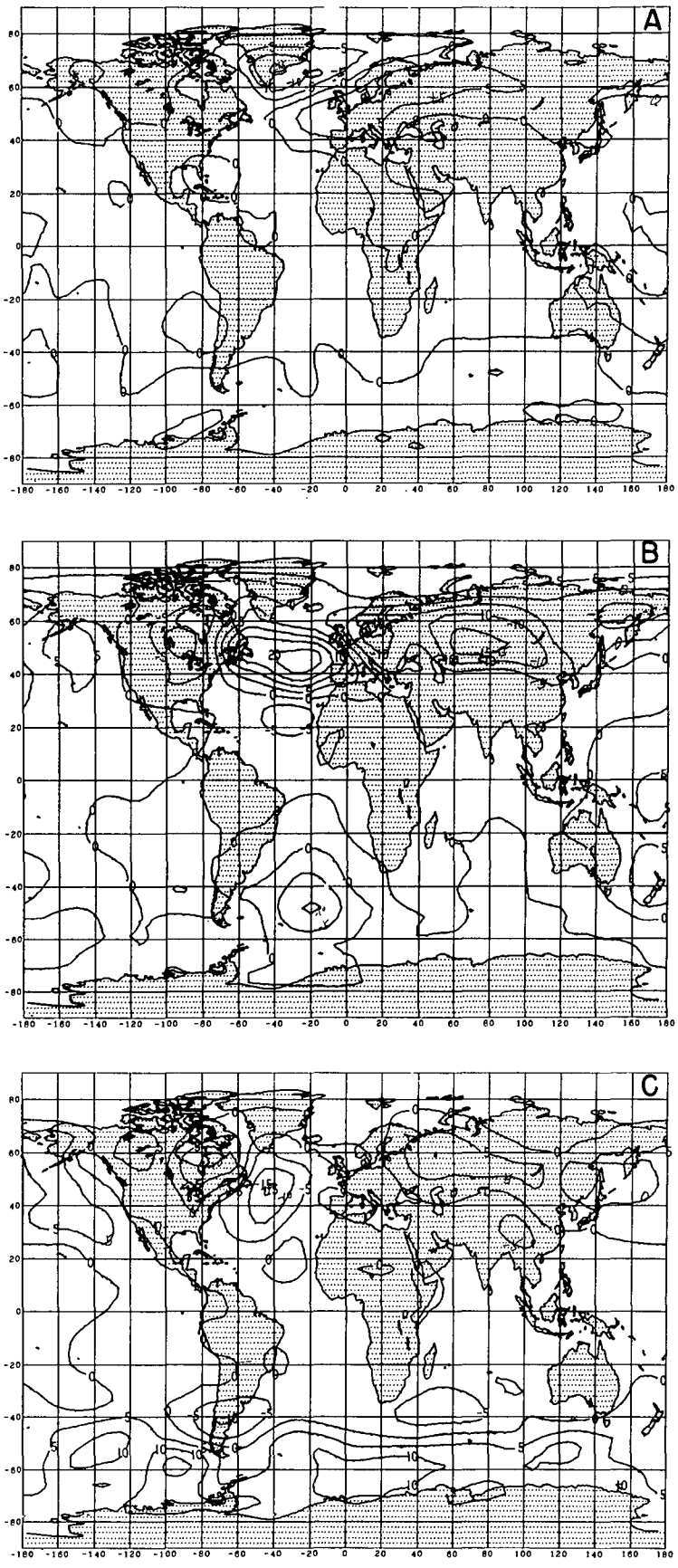

Fig. 21. Thirty-day mean sea level pressure difference maps (anomaly-minus-control) for experiment SNW-N. (A) 1-30 days; (B) 31-60 days; (C) 61-90 days.

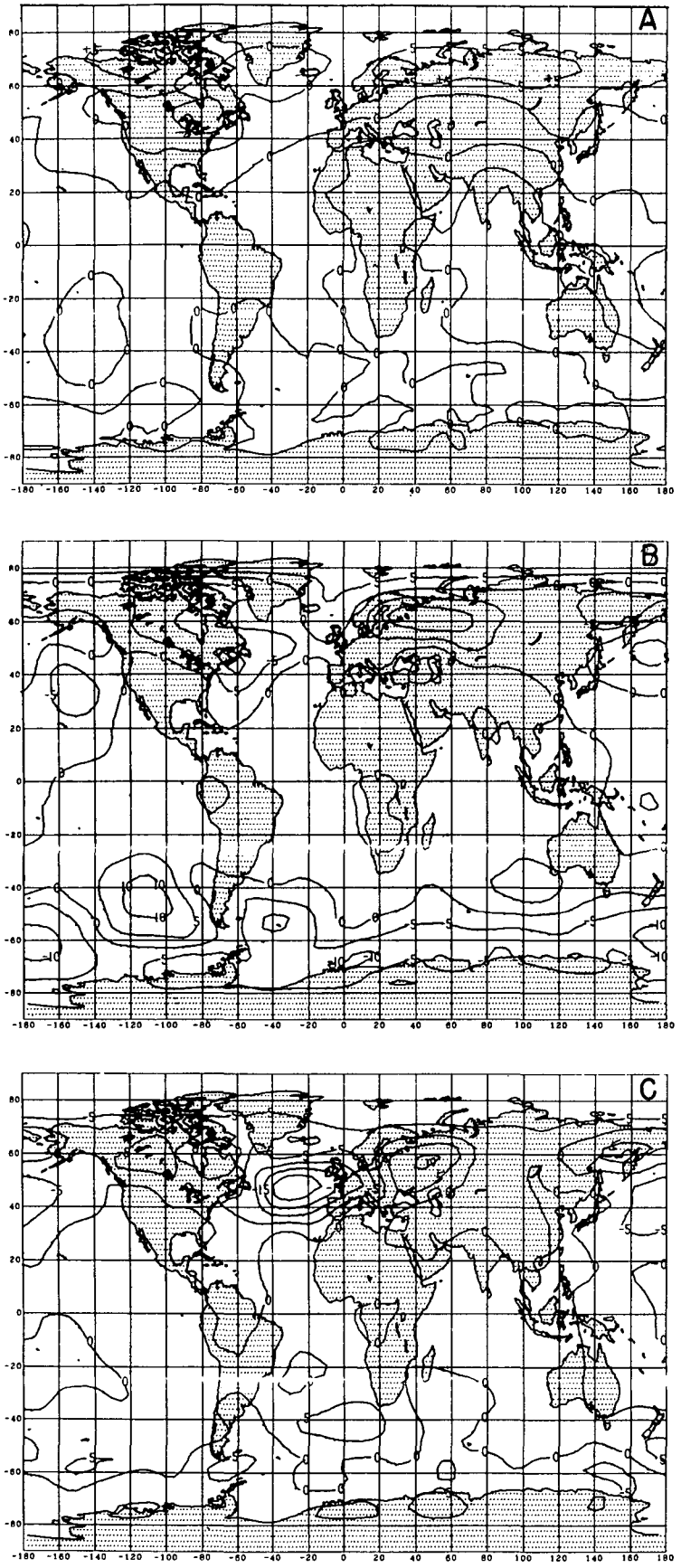

Fig. 22. Thirty-day mean sea level pressure difference maps (anomaly-minus-control) for experiment SNW-S. (A) 1-30 days; (B) 31-60 days; (C) 61-90 days.

is still greater for SNW-S than for SNW-N. In the North Pacific Ocean, where the monsoonal effects in the model are weaker than in the Atlantic, SNW-S and SNW-N produce generally more consistent results, with oceanic pressures lowered in the former case and raised in the latter in all three months relative to the control.

The influence of the continental snow line on the east coastal pressure index, P, is illustrated in figure 23 in which are shown the time series for both the SNW-N and SNW-S experiments together with the winter control time series for comparison. The outstanding effect of the snow line shift is the alteration of the major east coast cyclone event which occurred on day 49 in the control run (Fig. 23-B), when P fell to 994 mb. In SNW-N (Fig. 23-A) this event is much weaker than in the control run (about 999 mb), and begins and ends more gradually, both effects possibly being results of weaker baroclinicity associated with the more northerly snow line. The SNW-S P series exhibits a slight decrease in the intensity of this cyclonic event (996 mb minimum) and a marked retardation in phase, with the minimum occurring 13 days later than in the control run. Other than this dramatic but puzzling change in the character of the P index time series, no other clear-cut, systematic changes are evident either in the original time series or in the power spectra of the three series (not shown).

The effect of the snow line shift on the regional zonal index Z, as seen in Figure 24, is most obvious after about 50 days. In this latter portion of the period the Z index drops to a minimum of 145 meters in the SNW-N case (fig. 24-A) compared with a minimum of 270 meters, about 13 days later, in SNW-S (fig. 24-B). (The Z-index for the control run is not reproduced here, but can be seen in figure 14-A.) Thus, the northward shift of the snow line has the effect of reducing the 30°N-50°N zonal index after a period of about two months. As in the case of the P-index, the power spectra of the Z time series did not reveal any systematic pattern of differences between SNW-N and SNW-S.

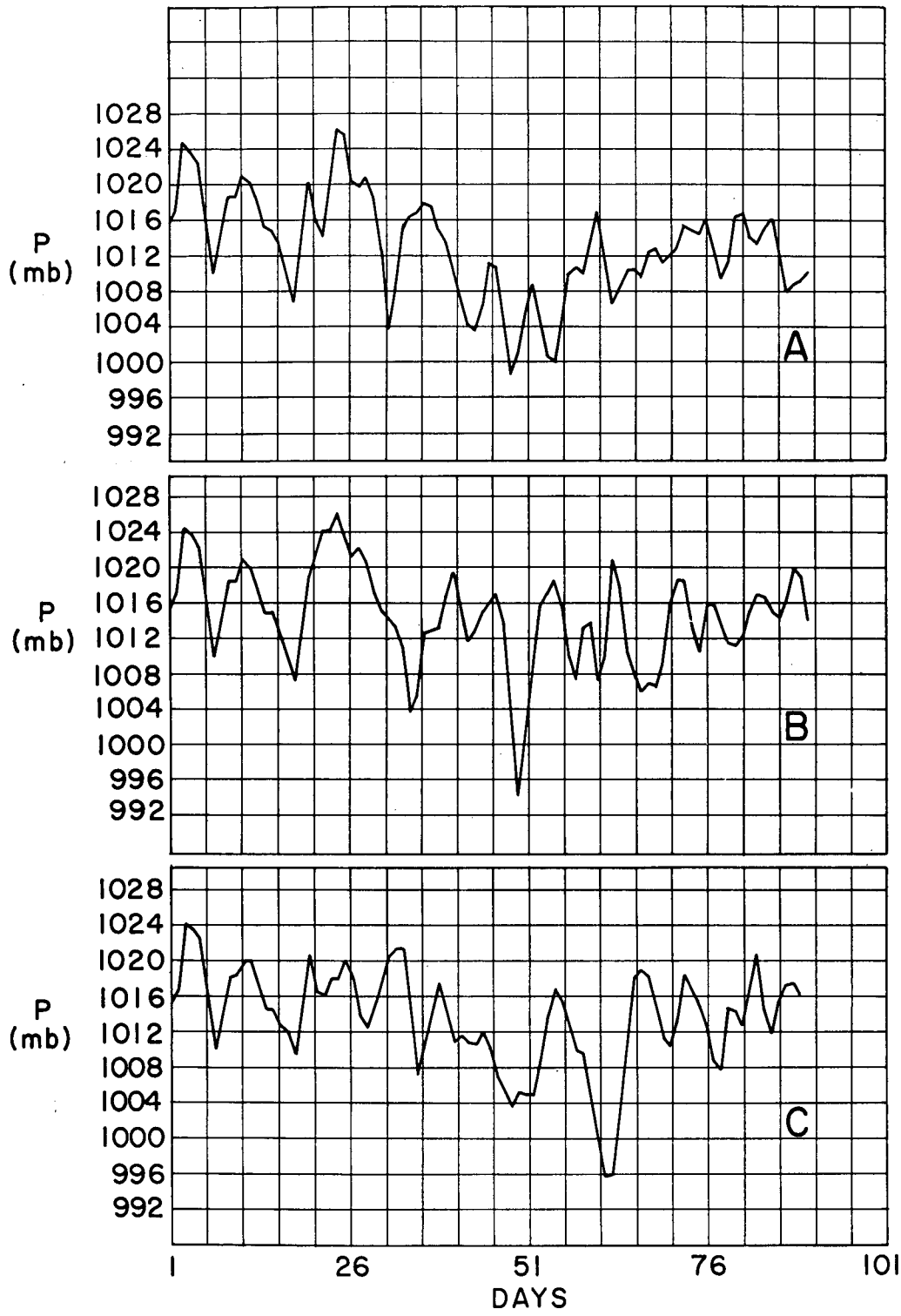

Fig. 23. Ninety-day time series of P index for (A) SNW-N, (B) winter control, and (C) SNW-S.

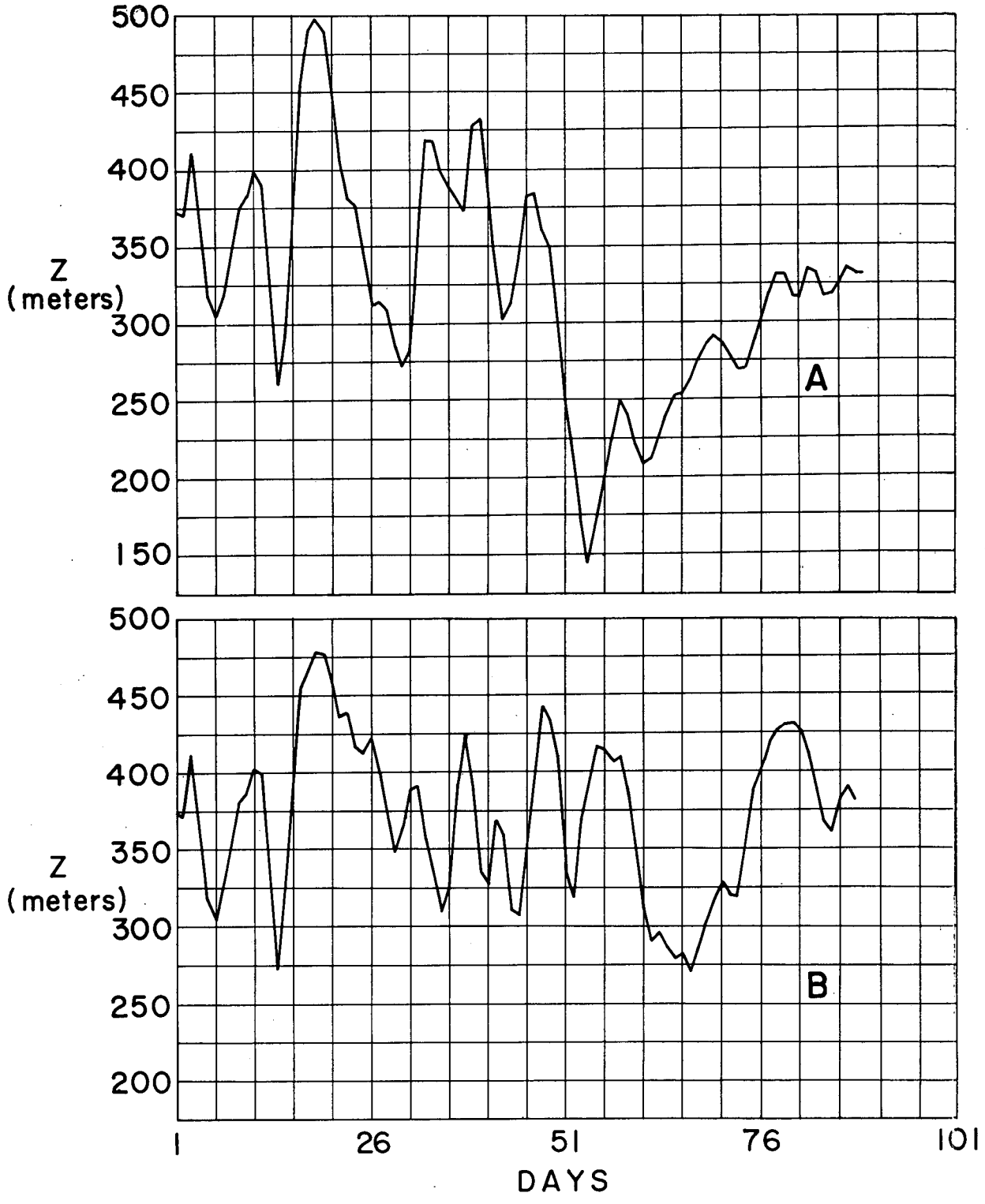

Fig. 24. Ninety-day time series of Z-index for (A) SNW-N and (B) SNW-S experiments.

Only in the case of the M-index is there strong evidence of a change in the spectral distribution of variance. As illustrated in figure 25, the southward shift of the snow line hardly altered the M power spectrum (smoothed and with linear trend removed), except for an increase of energy at the lowest frequencies (periods ≥ 10 days). However, the northward shift of the snow line was accompanied by a marked shift in spectral energy from high to low frequencies, with energy increasing relative to control at periods ≥ 4 days and decreasing at periods ≤ 3.3 days.

It is difficult to summarize neatly the results of the SNW experiment. Even the expected monsoonal effect on the sea level pressure field did not appear in unambiguous form, particularly in the North Atlantic. As to the regional index changes, no simple generalizations beyond the descriptions already given can be ventured.

Conclusions

The experiments described above have yielded results which could hardly have been anticipated. They indicate how difficult it is to make reliable estimates on the basis of qualitative reasoning of the dynamical consequences for the atmosphere of even the simplest alterations in surface conditions. Although the results of model calculations cannot be regarded as necessarily true for the atmosphere, it is unlikely that the solutions of the atmosphere will be less complicated than those of the model, or more predictable. Thus, the experiments should discourage efforts to guess what the dynamical effects on the atmosphere of any given surface anomalies might be. At the same time they point to the need for much more numerical experimentation, and for the development of more realistic models of the general circulation.

From the viewpoint of long range weather prediction, some notable results of the model experiments are: (1) a slow and generally unsystematic response of the atmosphere to anomalous sea surface temperatures in summer; (2) relatively rapid dynamical reactions to the same anomalies in winter, with marked interhemispheric effects

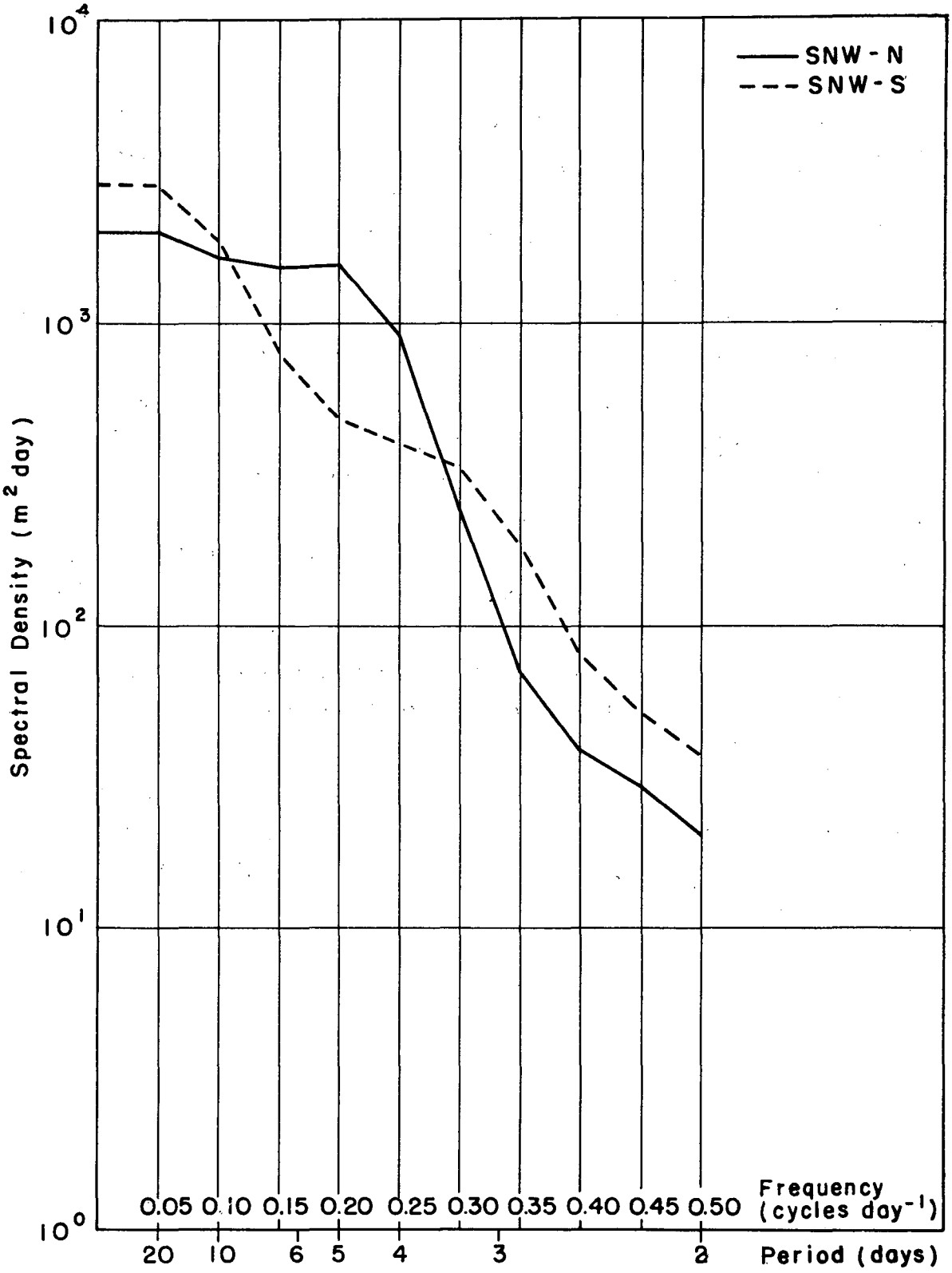

Fig. 25. Power spectra of M-index time series for (A) SNW-N and (B) SNW-S. The quadratic trend has been removed, and the spectra are smoothed over 3 cycles.

on the sea level pressure field after one month; (3) the failure of either the snow line or sea surface temperature anomalies to alter the spectral distribution of the various indices of synoptic activity in any systematic and unambiguous manner; (4) marked changes in the time of occurrence of major meteorological events, including phase shifts of one to two weeks in deep cyclone events, induced both by sea temperature and snow line alterations; and (5) a lack of symmetry between the transequatorial effects of Northern Hemisphere and Southern Hemisphere sea surface temperature anomalies.

In these experiments no attempt has been made to diagnose in detail the complex manner in which regional changes in baroclinicity resulting from sea temperature and snow cover alterations lead to global changes in the pressure distribution. Although it is apparent that an important link in the chain of developments is the hydrostatic tilting of isobaric surfaces resulting from anomalous horizontal heating gradients (otherwise known as "generation of available potential energy"), the subsequent mass adjustments (associated with transformations from potential to kinetic energy) occur in a manner that defies simple description.

Finally it must be reiterated that as yet we do not know either how model dependent these results are, or how closely they would simulate the behavior of a real atmosphere with identical initial conditions.

References

Arakawa, A., A. Katayama, and Y. Mintz, 1968: Numerical simulation of the general circulation of the atmosphere. Proceedings of the WMO/IUGG Symposium on Numerical Weather Prediction, Tokyo, 1968, pp. IV-7 to IV-8-12.

Bjerknes, J., 1966: A possible response of the atmospheric Hadley circulation to equatorial anomalies of ocean temperatures. Tellus, 18, 820-829.

Bjerknes, J., 1969: Atmospheric teleconnections from the equatorial Pacific. Monthly Weather Review, 97, 163-172.

Charney, J. C., et al., 1966: The Feasibility of a Global Observation and Analysis Experiment. National Academy of Science-National Research Council. Publication No. 1290, Washington, D. C. 172 pages.

Holloway, J. L., Jr. and S. Manabe, 1971: Simulation of climate by a global general circulation model. Monthly Weather Review, 99, 335-370.

Kasahara, A., and W. M. Washington, 1967: NCAR global general circulation model of the atmosphere. Monthly Weather Review, 95, 389-402.

Katayama, A., Y. Mintz, and A. Arakawa, 1971: Seasonal variations of the general circulation in a numerical simulation of the atmosphere. Department of Meteorology, U. C. L. A.

Langlois, W. E., and H. C. W. Kwock, 1969: Description of the Mintz-Arakawa numerical general circulation model. Tech. Rep. No. 3, Numerical Simulation of Weather and Climate. Dept. of Meteorology, U. C. L. A. 95 pages.

Leith, C. E., 1965: Numerical simulation of the earth's atmosphere. Methods in Computational Physics, vol. 4, Academic Press, pp. 1-28.

Manabe, S., and K. Bryan, 1969: Climate and the ocean circulation. Monthly Weather Review, 97, 739-827.

Mintz, Y., 1965: Very long-term global integration of the primitive equations of atmospheric motion. WMO Technical Note No. 66, World Meteorological Organization, pp. 141-161.

Namias, J., 1962: Influences of abnormal surface heat sources and sinks on atmospheric behavior. Proceedings of the Int'l Symposium on Numerical Weather Prediction in Tokyo, Nov. 7-13, 1960. pp. 615-627.

Namias, J., 1969: Seasonal interactions between the North Pacific Ocean and the atmosphere during the 1960's. Monthly Weather Review, 97, 173-192.

Namias, J., 1970: Temporal coherence in North Pacific sea-surface temperature patterns. Journal of Geophysical Research, 75, 5952-5955.

Namias, J., 1971: The 1968-69 winter as an outgrowth of sea and air coupling during antecedent seasons. Journal of Physical Oceanography, 1, 65-81.

Smagorinsky, J., S. Manabe, and J. L. Holloway, Jr., 1965: Numerical results from a nine-level general circulation model of the atmosphere. Monthly Weather Review, 93, 727-768.